AD NUMBER

AD811673

NEW LIMITATION CHANGE

TO

Approved for public release, distribution unlimited

FROM

Distribution authorized to U.S. Gov't. agencies only; Administrative/Operational use; Sep 1966. Other requests shall be referred to Commanding Officer, U.S. Army Ballistic Research Laboratories, Aberdeen Proving Ground, MD.

AUTHORITY

USAARDC ltr, 27 Dec 1977.

THIS REPORT HAS BEEN DELIMITED
AND CLEARED FOR PUBLIC RELEASE
UNDER DOD DIRECTIVE 5200.20 AN
NO RESTRICTIONS ARE IMPOSED UP
ITS USE AND DISCLOSURE.

DISTRIBUTION STATEMENT A

APPROVED FOR PUBLIC RELEASE;
DISTRIBUTION UNLIMITED.

BRL R 1344

AD

BRL

811673

REPORT NO. 1344

AIR BLAST PARAMETERS VERSUS DISTANCE FOR HEMISPHERICAL TNT SURFACE BURSTS

by

C. N. Kingery

September 1966

U. S. ARMY MATERIEL COMMAND
BALLISTIC RESEARCH LABORATORIES
ABERDEEN PROVING GROUND, MARYLAND

B A L L I S T I C   R E S E A R C H   L A B O R A T O R I E S

REPORT NO. 1344

SEPTEMBER 1966

This document is subject to special export controls and each transmittal to foreign governments or foreign nationals may be made only with prior approval of Commanding Officer, U.S. Army Ballistic Research Laboratories, Aberdeen Proving Ground, Maryland

AIR BLAST PARAMETERS VERSUS DISTANCE FOR HEMISPHERICAL TNT SURFACE BURSTS

C. N. Kingery

Terminal Ballistics Laboratory

Program was supported in part by the Defense Atomic Support Agency; Subtask No. 01.049.

A B E R D E E N   P R O V I N G   G R O U N D,   M A R Y L A N D

BALLISTIC RESEARCH LABORATORIES

REPORT NO. 1344

CNKingery/sjw
Aberdeen Proving Ground, Md.
September 1966

AIR BLAST PARAMETERS VERSUS DISTANCE FOR HEMISPHERICAL TNT SURFACE BURSTS

ABSTRACT

This report contains a presentation of the air blast parameters, peak overpressure, arrival time, positive duration and impulse versus scaled distances. The values of the parameters are derived from empirical measurements made on a series of tests sponsored under The Technical Cooperation Program (TTCP) i.e., Canada, the United Kingdom and the United States. The measurements were made on 5-, 20-, 100- and 500-ton TNT surface bursts. The charges consisted of small TNT blocks stacked in the shape of a hemisphere.

PREVIOUS PAGE WAS BLANK, THEREFOR WAS NOT FILMED.

TABLE OF CONTENTS

PREVIOUS PAGE WAS BLANK, THEREFOR WAS NOT FILMED.

SYMBOLS AND ABBREVIATIONS

D	Distance from ground zero (GZ)
W	Yield of weight of explosive charge in pounds
λ	Scaled distance from ground zero (scaled to one pound at sea level) or $D/W^{1/3}$
t_a	Arrival time of the blast wave at D
t_{as}	Scaled time of arrival
ΔP	Positive peak overpressure
ΔP_s	Scaled positive peak overpressures
$t+$	Positive duration
t_{+s}	Scaled positive duration
I	Positive impulse
I_s	Scaled positive impulse
P_o	Atmospheric pressure at sea level (14.7 psi)
P_a	Ambient atmospheric pressure at test site
T_o	Temperature at sea level (15 C)
T_a	Ambient temperature at test site
C_o	Sound velocity at sea level (1116.4 ft/sec)
U	Velocity of shock front
σ	Ratio of specific heats
M	Mach Number U/c_o
e	Experimental
c	Computed

SYMBOLS AND ABBREVIATIONS (Contd)

The curves and tabulations presented in this report are scaled to standard sea level atmospheric conditions for the yield of a one-pound TNT hemispherical charge fired on the surface. To use the curves or tabulations for predicting the blast parameters under other atmospheric conditions and charge weights the following scaling factors should be used. That is, multiply the values presented in this report by the scaling factors obtained from the following equations:

$S_p = (\frac{P_a}{P_o})$ Pressure scaling factor

$S_d = (W)^{1/3} (\frac{P_o}{P_a})^{1/3}$ Distance scaling factor

$S_t = (W)^{1/3} (\frac{P_o}{P_a})^{1/3} (\frac{288}{T_a + 273})^{1/2}$ Time scaling factor

$S_i = (W)^{1/3} (\frac{P_a}{P_o})^{2/3} (\frac{288}{T_a + 273})^{1/2}$ Impulse scaling factor

Where W in the above equations is the charge weight for which the blast parameters are being predicted.

INTRODUCTION

This report is a compilation of experimental data measured on a series of TNT detonations. The results have been carefully analyzed and presented in a useful form for the engineer or experimenter. The objective of this report is to present the experimental determinations of certain blast parameters. These parameters were measured from records obtained from the surface detonations of TNT hemispheres ranging from 5 to 500 tons. They have been reduced to a yield of one pound of TNT detonated at standard sea level conditions. The scaled values are tabulated and presented in the form of blast parameter versus distance. This report is a follow-on to an earlier report[1*] containing tabulations and a curve of peak overpressure versus distance.

BACKGROUND

The Ballistic Research Laboratories (BRL) have participated with the Suffield Experimental Station (SES), a facility of the Canadian Defense Research Board, in a series of multi-ton TNT experiments starting in 1959. In these experiments the BRL, in addition to conducting various effects and target response projects have always instrumented a blast line to measure the pressure-time history of the blast wave at selected radial distances from ground zero. BRL participated in a 5-ton test in 1959, a 20-ton test in 1960, a 100-ton test in 1961 and a 500-ton test in 1964. On the last three tests, the U.S. participation was under the sponsorship of the Defense Atomic Support Agency (DASA) and the guidance of The Technical Cooperation Program (TTCP). Under the TTCP the United Kingdom, Canada and the United States all participated in a coordinated program.

The experimental test area at SES covers approximately one thousand square miles of undulating prairie. The earth medium at the test site is a glacially deposited silt with underlying clay, sand, and gravel. The general terrain is quite level and ideally suited for multi-ton surface bursts.

---

[*] *Superscript numbers denote references which may be found on page 69.*

The charges were constructed in a hemispherical configuration with the flat side resting on the surface. They consisted of 12 x 12 x 4 inch blocks of cast TNT (density 1.56 gm/cc); each block weighed 32.6 lbs $\pm$ 0.063 lbs. A photograph of the 500-ton charge is shown in Figure 1.

A description of the first three tests and source references are presented in Reference 1.

The 500-ton shot "Operation SNOW BALL" is described in a two-volume preliminary report,[2] and a two-volume report on symposium precedings.[3]

PROCEDURE

The data from all four tests were first processed to obtain the "as read" values of peak overpressure, arrival time, positive duration and positive impulse. The cube root scaling and altitude corrections were applied to these values to bring them to standard sea-level conditions and the equivalent of a one-pound charge. The scaled values were then used to determine the curves presented in this report. The method used to determine the "best fit" curve is described for each parameter.

Arrival Time

The arrival time of the blast wave is defined as that interval of time between the initiation of the detonator caps and the arrival of the blast wave at a specific distance. Therefore, the arrival time includes the detonation time. Arrival time may be measured by several methods.

One method is the use of high speed cameras to photograph the fire ball and the shock front as it propagates radially from the surface of the charge. The almost discontinuous change in pressure, density and temperature at the shock front causes a similar change in the refractive index of air. Therefore when a black and white striped backdrop is viewed through the region immediately behind the shock front, the rays of light are deflected and a distortion or discontinuity in the backdrop pattern is apparent. The passage of the shock wave, as revealed by the propagation of the discontinuities can be photographed. Each frame of

FIGURE 1 500-TON TNT HEMISPHERICAL CHARGE the film records the new position of the shock front and a large number of small time intervals are recorded; thus we are provided with an accurate radius-time history of the shock front. A variation of the backdrop technique is to photograph the deflection of trails of smoke rockets fired just prior to the detonation. The deflection caused by the passage of the shock can be recorded and thereby the radius of the shock front can be established from the high speed motion pictures.

A second method used during the series of tests was a direct measurement using blast switches which produced signals when struck by the shock front. The switches were placed at selected radial distances and when struck each gage provided an electrical signal which was recorded as a function of time.

Overpressure gauges also measured the arrival time of the blast wave and were used to supplement other methods. This should be considered a variation of the blast switch technique rather than a new method.

A third method involves the use of coaxial cable (slifer cable) which shorts out when exposed to high overpressures. To measure blast wave arrival times the cable is laid along the surface of the ground from the detonation point out to a point where the predicted overpressure is less than the pressure required to crush the cable. A Colpitts oscillator is connected to the cable; as the blast wave progresses along the cable, the cable collapses, thus changing the circuit inductance (and frequency) continuously. By proper calibration of the system the oscillator frequency as a function of inductance (cable length) will be known, thus the location of the crushing force can be determined at any point along the cable. See Reference 5 for a detailed description and results obtained on Operation SNOW BALL.

Velocity

The velocity of the shock front (U) associated with a blast wave is not recorded as a direct measurement but must be calculated from the arrival time versus distance data.

$$U = \frac{d\lambda}{dt_{as}} \quad . \tag{1}$$

The primary reason for measuring arrival time is to gather data necessary to determine the velocity of the shock front at selected distances. Determining the shock front velocity enables one to derive the peak overpressure from the Rankine-Hugoniot relationship:[7]

$$\frac{\Delta P_s}{P_o} = \left(\frac{U}{C_o}\right)\left(\frac{u}{C_o}\right)(1.4) \tag{2}$$

A detailed treatment of the methods and problems associated with determining peak overpressure from measurements of arrival time is presented in Reference 4.

Peak Overpressure

The determination of peak overpressures measured on the 5-, 20- and 100-ton tests is discussed in Reference 1. The overpressure-distance curve from that report was modified to include close-in higher overpressure values and is presented in this report to provide a complete presentation of the available measured parameters. The peak overpressures were obtained from direct measurements provided by pressure sensitive transducers and the arrival time-velocity calculations using the Rankine-Hugoniot relationship. Better close-in arrival time data and overpressure measurements were obtained on the 500-ton test than on the previous shots; therefore, the peak overpressure versus distance curve is updated to include the results from the 500-ton test.

Positive Duration

Positive duration is defined as that interval of time between the arrival of the positive pressure pulse associated with the blast wave and the end of the positive pressure pulse, or a return to the ambient pressure conditions. The positive durations presented in this report were obtained from recordings of the pressure-time history of the blast wave using pressure sensitive transducers with time-calibrated recording systems.

Positive duration is very difficult to measure with consistency and repeatability. The measured records values are very susceptible to gage hysteresis, base line drift, and fluctuations due to acceleration-sensitive gages. Where there was some discrepancy in individual measurements, the data from the pressure-time record was plotted on semi-log graph paper and extrapolated to zero overpressure. Plotting the pressure on the linear scale and the time on the log scale tends to give a straight line graph and a better interpolated value for duration.

Positive Impulse

The positive impulse of the blast wave is the integrated area under the pressure-time curve and is important in relating target damage to yield and overpressure. Since the impulse is an integrated area and expressed in psi-msec, the computed value is a function of the overpressure, the positive duration and the rate of decay behind the shock front. When a record of deflection (where deflection is a function of pressure) versus time is analyzed and programmed in the computer to obtain pressure versus time, the computer is also programmed to integrate the data and tabulate impulse. The impulse values as read from the individual records were scaled to a 1 pound TNT charge at standard sea level conditions.

PRESENTATION OF DATA

Comments are made on the results of each shot and the data are presented in the form of curves and tabulations. The report presents only scaled values of the various parameters.

Initially twelve curves were drawn. These were scaled positive duration, scaled positive impulse, and scaled arrival time. Each parameter was plotted as a function of scaled distance from ground zero for each of the four detonations. This separation of the tests was carried out to allow the detection of any trends related to yield and to test the scaling methods.

Certain trends were evident when direct comparisons were made between the scaled values from the different yields. These trends will be discussed as the various parameters are presented. The curves established for each yield were drawn by visual inspection of the data points. Because of the many inflections in the positive duration and positive impulse curves, no least squares fits were attempted. In the case of the arrival time curve, the data were in such excellent agreement that a least-squares fit was used only for the close-in values.

Method of Analysis

Because of the large amount of scatter in the positive duration and positive impulse data, it was necessary to perform a thorough review of all pressure records in order to eliminate faulty data.

Several methods were used to distinguish between "good" and "bad" records. All records exhibiting excessive noise or oscillations were disregarded. Slow rise times, hysteresis and non-uniformity of recording running speed were the most common causes of defective records. As a final check the peak overpressure of each record was compared to the standard pressure-distance curve presented in Reference 1. In this manner it was possible to sift out "bad" records caused by faulty transducers or calibration techniques. This review eliminated approximately 20 percent of the records. The data thus retained were reasonable and consistent.

Because of the limited number of points and the inflections along the positive duration and positive impulse curve, it appeared impractical to use any of the standard least-squares fitting techniques to derive an equation describing the duration or impulse as a function of distance. Therefore, these curves were drawn to best represent the data by visual inspection.

After establishing a hand drawn curve there was still a requirement to know how well the curve represented the data, that is, the distance and number of points above and below the curve or a determination of the relative error. To answer these questions a system of data analysis was devised which provides a clear picture of the dependability of the curves. This method was also applied to the arrival time data even though the curve had no inflections.

Following are the definitions of the important quantities which apply to all three curves:

- Relative Error: A relative error is assigned to each experimental point. Relative error is defined by the following equation:

$$R.E. = \frac{Y - Yo}{Yo} \qquad (3)$$

  where Y is the ordinate of the point and Yo is the ordinate of the standard or established curve at the the same scaled distance from ground zero. Relative error is denoted by the symbol R.E.

- Average Relative Error: An average relative error is assigned to the data points used to determine each curve. It is defined as the sum of the relative errors (with signs included) of all the points , divided by the number of points used to determine the particular curve. This provides a quantative indication of how close the curve comes to the "middle" of the points. Average relative error is denoted by the letters A.R.E.

- Average Absolute Relative Error: Each curve is assigned an average absolute relative error for the points used in its determination. The average absolute relative error is defined as the average of the absolute values of the relative errors. This quantity indicates the amount of scatter of the points about the curve. Average absolute relative error is denoted by the letters A.A.R.E.

- Average Positive Relative Error: The average positive relative error is defined as the average relative error of all points above the curve and is denoted by the letters A.P.R.E.

- Average Negative Relative Error: The average negative relative error is defined as the average relative error of all points below the curve and is denoted by the letters A.N.R.E.

- Number Positive Points: The number of points above the constructed curve is abbreviated as N.P.P.

- Number Negative Points: The number of points below the constructed curve is abbreviated as N.N.P.

TABULATIONS AND CURVES

In this section the scaled data points for each shot are tabulated and a curve representing those points is presented for each parameter being considered. A composite curve has been developed and is presented along with a tabulation of the relative errors of the points used to determine the curve.

Positive Duration Curves

The development of the positive duration curve begins with a tabulation of scaled data points of the positive duration recorded on the 5-, 20-, 100- and 500-ton TNT detonations. The data points were taken from selected pressure-time records which met the established criterion for "good" records. Tables I through IV include the scaled positive duration versus scaled distance from ground zero for the 5-, 20-, 100- and 500-ton TNT detonations respectively. Curves representing the tabulations are presented in Figures 2 through 5.

The scaled values of positive duration for the 5-ton and 20-ton shot are presented in Tables I and II. Figures 2 and 3 are curves drawn from visual inspection of the data contained in those tables. A comparison between the two curves show a similar shape, but the curve for the 20-ton shot is consistently lower out to about 8λ. No explanation to account for this difference is offered at this time.

TABLE I

SCALED POSITIVE DURATION AND DISTANCE VALUES FOR
A 5-TON TNT DETONATION

λ	t_{+s}	λ	t_{+s}
$FT/LBS^{1/3}$	$MSEC/LBS^{1/3}$	$FT/LBS^{1/3}$	$MSEC/LBS^{1/3}$
1.49	.34	7.46	2.44
1.72	.44	7.46	2.44
2.26	1.24	9.49	2.71
2.26	1.26	20.34	3.93
3.16	1.81	35.62	4.50
3.16	2.03	42.49	4.28
3.16	2.14	42.49	4.28
4.75	1.62	42.49	4.36
4.75	1.71	81.36	5.19
4.75	1.81	81.36	5.19
4.75	1.81	81.36	5.42
4.75	1.99	81.36	5.42
6.01	1.85	153.70	5.64
6.01	1.94	153.70	6.32
7.46	2.26	316.40	8.15
7.46	2.35	316.40	6.32

FIG. 2 SCALED POSITIVE DURATION VS SCALED DISTANCE FOR A 5 TON TNT DETONATION

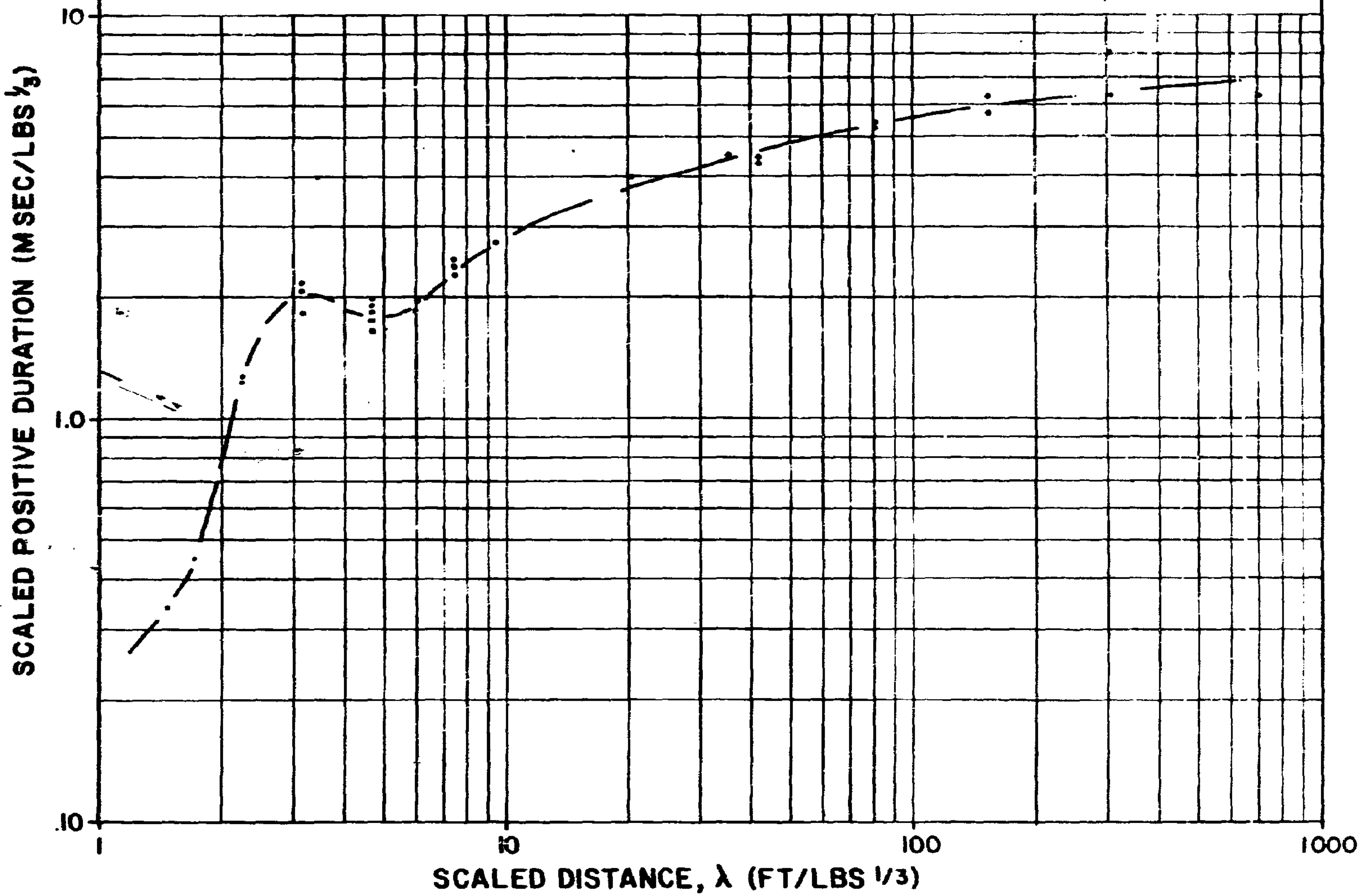

TABLE II

SCALED POSITIVE DURATION AND DISTANCE VALUES FOR
A 20-TON TNT DETONATION

λ	t_{+s}	λ	t_{+s}
$FT/LBS^{1/3}$	$MSEC/LBS^{1/3}$	$FT/LBS^{1/3}$	$MSEC/LBS^{1/3}$
1.14	.19	8.28	2.33
1.14	.20	8.28	2.51
1.28	.16	8.28	2.58
1.28	.23	11.71	2.76
2.34	1.03	11.71	2.83
2.34	1.27	11.71	2.99
3.11	1.13	11.71	3.03
3.11	1.25	11.71	3.04
3.11	1.33	17.56	3.17
3.11	1.56	17.56	3.26
3.11	1.62	17.56	3.24
4.20	1.25	17.56	3.28
4.20	1.27	17.56	3.35
4.20	1.29	17.56	3.41
4.20	1.32	17.56	3.42
4.20	1.64	35.13	4.09
4.20	1.88	35.13	4.16
4.20	1.91	58.55	4.20
5.77	1.51	58.55	4.55
5.77	1.58	35.13	4.70
5.77	1.60	199.90	6.02
5.77	1.62	199.90	6.76
5.77	1.72	428.40	7.60
5.77	1.94	428.40	8.05
8.28	2.19	428.40	8.34
8.28	2.24	428.40	8.34
8.28	2.27	428.40	8.43
8.28	2.32		

FIG. 3 SCALED POSITIVE DURATION VS SCALED DISTANCE FOR A 20 TON TNT DETONATION

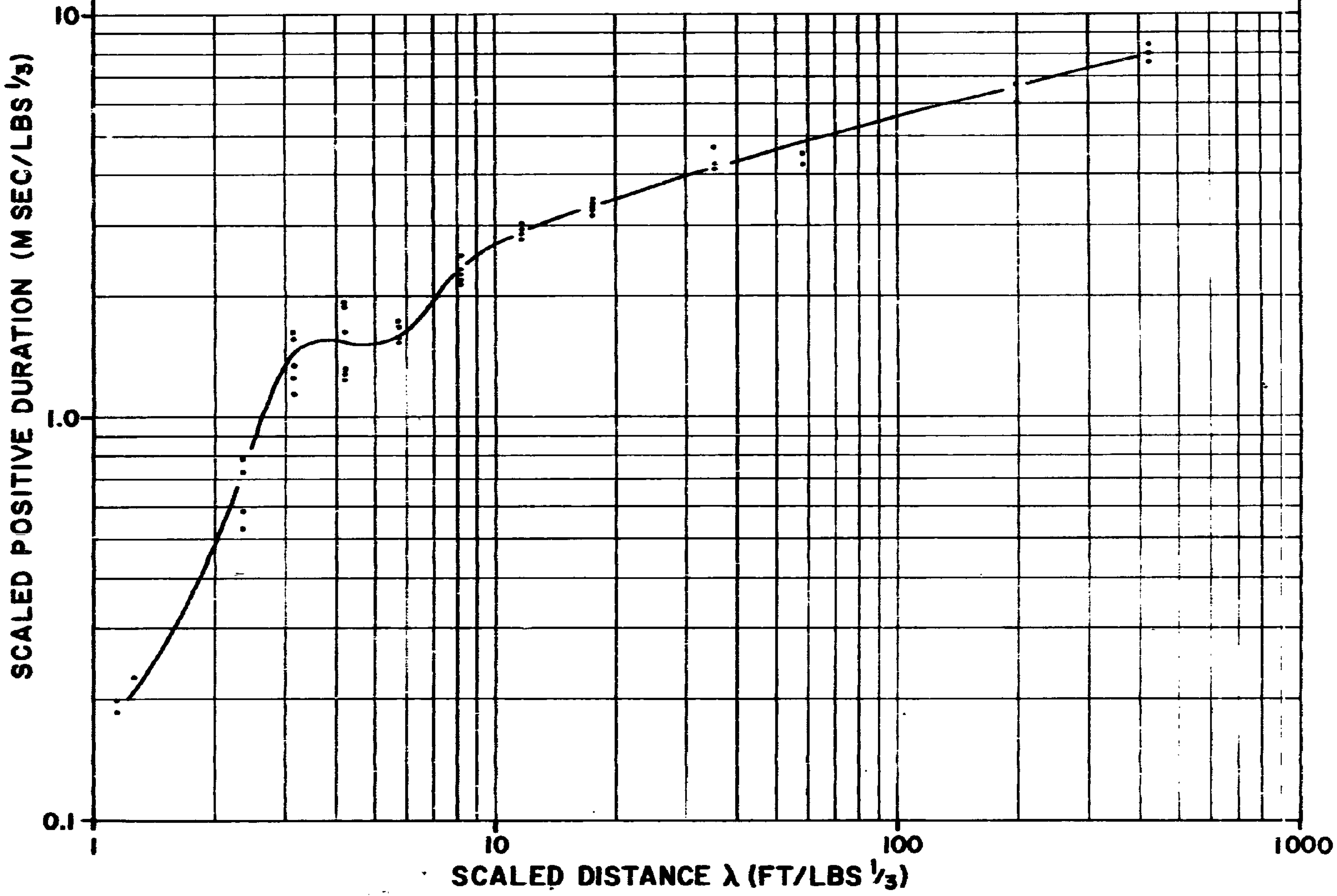

TABLE III

SCALED POSITIVE DURATION AND DISTANCE VALUES FOR A 100-TON TNT DETONATION

λ	t_{+s}	λ	t_{+s}
FT/LBS$^{1/3}$	MSEC/LBS$^{1/3}$	FT/LBS$^{1/3}$	MSEC/LBS$^{1/3}$
3.40	1.30	7.39	2.10
4.36	1.74	7.76	1.86
4.66	2.00	8.76	2.26
4.99	1.69	9.51	2.51
5.02	1.64	14.07	3.03
5.02	1.67	17.02	3.15
5.57	2.10	46.73	4.30
6.11	1.87	46.73	4.33
6.84	2.09	116.80	5.74
6.89	1.74	116.80	5.81
6.89	1.81	166.90	5.71
6.89	2.04	166.90	5.83
7.39	2.04	250.40	6.09
7.39	2.09		

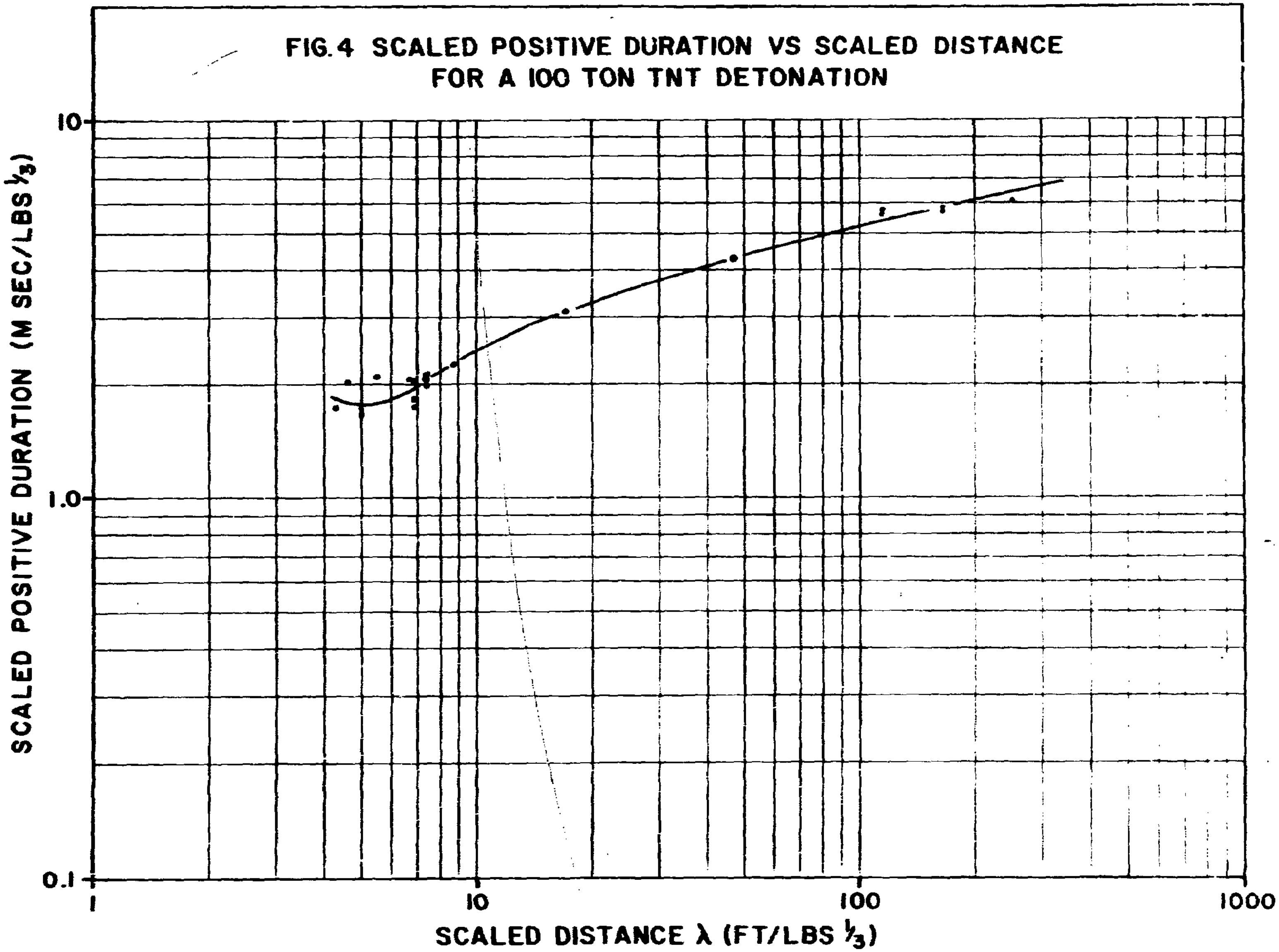

FIG.4 SCALED POSITIVE DURATION VS SCALED DISTANCE
FOR A 100 TON TNT DETONATION
SCALED POSITIVE DURATION (M SEC/LBS 1/3)
10
1.0
0.1
1
10
100
1000
SCALED DISTANCE λ (FT/LBS 1/3)

TABLE IV

SCALED POSITIVE DURATION AND DISTANCE VALUES FOR A 500-TON TNT DETONATION

λ	t_{+s}	λ	t_{+s}
$FT/LBS^{1/3}$	$MSEC/LBS^{1/3}$	$FT/LBS^{1/3}$	$MSEC/LBS^{1/3}$
.49	.19	5.55	1.56
.79	.18	6.13	1.26
1.71	.29	6.72	2.01
2.97	1.33	7.80	1.76
2.97	1.56	7.80	2.11
3.46	1.31	7.80	2.31
4.14	1.23	9.35	2.23
3.46	1.36	9.35	2.31
4.53	1.36	14.10	2.76
5.55	1.27	99.00	5.22

FIG. 5 SCALED POSITIVE DURATION VS SCALED DISTANCE FOR A 500 TON TNT DETONATION

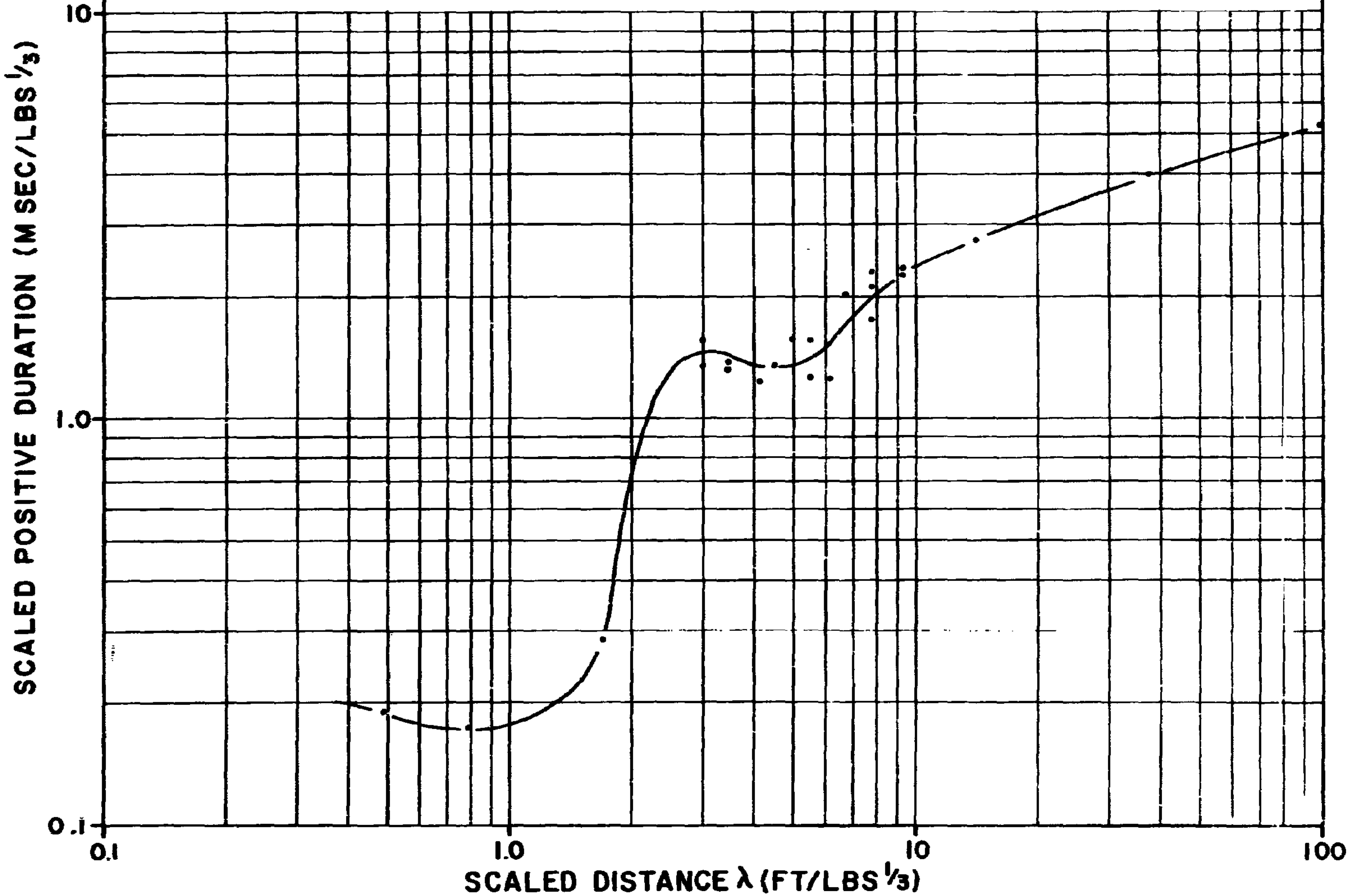

The scaled values of positive duration presented in Table III for the 100-ton shot are plotted in Figure 4. This curve was drawn to best fit the data and also follows the trend established from the 5- and 20-ton shots. The overall curve is lower than the 5-ton curve except for the dip at 5λ, where the two curves coincide over a short ground range. The general shape of the 20- and 100-ton curves is similar but no definite trend can be established, other than to say that the 100-ton values are slightly lower at distances greater than 7λ.

The scaled values of positive duration listed in Table IV for the 500-ton shot have been plotted in Figure 5. The curve drawn through the points follow the trend already established from the lower yield shots. With the exception of one point, the 100-ton curve is higher at λ's less than 8. At distances greater than 8λ the 100-ton and 500-ton curves coincide. The 500-ton and 20-ton curve show good agreement in general shape but the 20-ton curve is slightly higher at distances greater than 4λ; whereas, the 5-ton curve is higher than the 500-ton curve over the full range of scaled distances presented.

In Figure 6 a composite curve has been drawn to best represent all data points. As noted above the scaled positive duration appears to be yield dependent and it is suggested that for yields of 10 tons or less that the scaled 5-ton curve be used. For yields greater than 10 tons the composite curve will probably best represent predicted durations.

All data points listed in Tables I through IV are presented in Table V as well as the values of positive duration obtained at similar λ's from the composite curve. The difference between the experimental values of positive duration and those obtained from the composite curve are also tabulated. From this difference, a relative error, is calculated which gives an indication of how well each point fits the curve and its location above or below the curve (i.e., positive or negative). The analysis of the data and the constructed curve produced the values listed below.

Number of Positive Points	66
Number of Negative Points	68
Total Number of Points	134

FIG. 6 COMPOSITE SCALED POSITIVE DURATION VS SCALED DISTANCE FOR 5,20,100 AND 500 TON TNT DETONATIONS

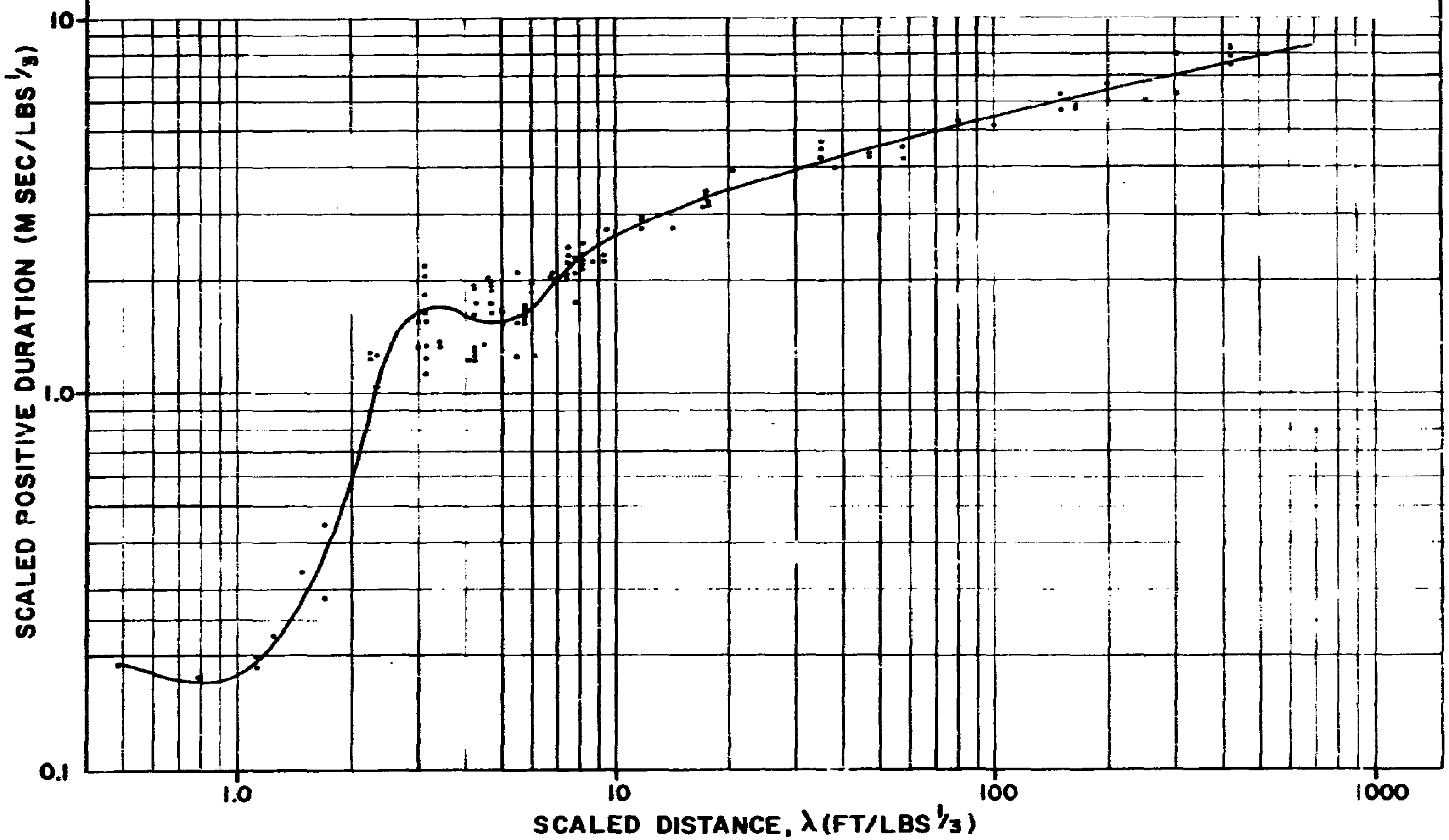

TABLE V

RELATIVE ERROR DETERMINATIONS FOR POSITIVE DURATION

λ	$\Delta^e t_{+s}$	$\Delta^c t_{+s}$	DIFF.	R. E.
.487	.1900	.1911	- .001	-.005652
.789	.1760	.1700	.006	.035294
1.142	.1998	.1976	.002	.011338
1.142	.1851	.1976	- .012	-.063069
1.285	.2262	.2267	.000	-.002206
1.285	.1586	.2267	- .068	-.300397
1.492	.3386	.2854	.053	.186239
1.710	.2860	.3805	- .094	-.248357
1.718	.4424	.3849	.058	.149389
2.260	1.2640	.9595	.305	.317353
2.260	1.2410	.9595	.282	.293382
2.342	1.0340	1.0886	- .055	-.050200
2.342	1.2660	1.0886	.177	.162908
2.970	1.5600	1.6495	- .089	-.054259
2.970	1.3300	1.6495	- .319	-.193695
3.113	1.6200	1.6781	- .058	-.034611
3.113	1.2510	1.6781	- .427	-.254505
3.113	1.1280	1.6781	- .550	-.327803
3.113	1.3310	1.6781	- .347	-.206832
3.113	1.5630	1.6781	- .115	-.068578
3.164	1.8060	1.6862	.120	.071022
3.164	2.0310	1.6862	.345	.204455
3.164	2.1400	1.6862	.454	.269096
3.405	1.3050	1.7000	- .395	-.232353
3.460	1.3100	1.7000	- .390	-.229412
3.460	1.3600	1.7000	- .340	-.200000
4.140	1.2300	1.6016	- .372	-.232018
4.198	1.9100	1.5981	.312	.195154
4.198	1.8800	1.5981	.282	.176382
4.198	1.2720	1.5981	- .326	-.204065
4.198	1.2480	1.5981	- .350	-.219082
4.198	1.6390	1.5981	.041	.025580
4.198	1.2950	1.5981	- .303	-.189673
4.198	1.3160	1.5981	- .282	-.176532
4.356	1.7400	1.5886	.151	.095276
4.530	1.3600	1.5794	- .219	-.138914
4.657	2.0010	1.5769	.424	.268978
4.746	1.8100	1.5751	.235	.149148
4.746	1.7150	1.5751	.140	.088834
4.746	1.9900	1.5751	.415	.263428
4.746	1.6250	1.5751	.050	.031694
4.746	1.8060	1.5751	.231	.146608

TABLE V (Contd)

RELATIVE ERROR DETERMINATIONS FOR
POSITIVE DURATION

λ	$\Delta^e t_{+s}$	$\Delta^c t_{+s}$	DIFF.	R. E.
4.990	1.6880	1.5702	.118	.075022
5.024	1.6700	1.5719	.098	.062395
5.024	1.6360	1.5719	.064	.040765
5.550	1.5600	1.6190	- .059	-.036442
5.550	1.2700	1.6190	- .349	-.215565
5.574	2.1050	1.6233	.482	.296725
5.769	1.6160	1.6584	- .042	-.025579
5.769	1.7210	1.6584	.063	.037735
5.769	1.5980	1.6584	- .060	-.036432
5.769	1.9420	1.6584	.284	.170994
5.769	1.5100	1.6584	- .148	-.089495
5.769	1.5770	1.6584	- .081	-.049095
6.012	1.9410	1.7031	.238	.139673
6.012	1.8510	1.7031	.148	.086829
6.109	1.8700	1.7283	.142	.081963
6.130	1.2600	1.7338	- .474	-.273273
6.720	2.0100	1.9092	.101	.052797
6.843	2.0880	1.9535	.135	.068862
6.893	1.7400	1.9715	- .231	-.117414
6.893	2.0360	1.9715	.065	.032727
6.893	1.8100	1.9715	- .161	-.081908
7.394	2.0360	2.1282	- .092	-.043323
7.394	2.0880	2.1282	- .040	-.018889
7.394	2.1050	2.1282	- .023	-.010901
7.459	2.2600	2.1477	.112	.052288
7.459	2.4380	2.1477	.290	.135168
7.459	2.3470	2.1477	.199	.092797
7.459	2.4380	2.1477	.290	.135168
7.761	1.8630	2.2279	- .365	-.163772
7.800	1.7600	2.2380	- .478	-.213584
7.800	2.3100	2.2380	.072	.032172
7.800	2.1100	2.2380	- .128	-.057194
8.282	2.5120	2.3464	.166	.070576
8.282	2.3350	2.3464	- .011	-.004859
8.282	2.1890	2.3464	- .157	-.067081
8.282	2.5850	2.3464	.239	.101688
8.282	2.3210	2.3464	- .025	-.010825
8.282	2.2740	2.3464	- .072	-.030856
8.282	2.2440	2.3464	- .102	-.043641
8.762	2.2620	2.4372	- .175	-.071871
9.350	2.2300	2.5360	- .306	-.120662
9.350	2.3100	2.5360	- .226	-.089117

TABLE V (Contd)

RELATIVE ERROR DETERMINATIONS FOR
POSITIVE DURATION

λ	$\Delta^e t_{+s}$	$\Delta^c t_{+s}$	DIFF.	R. E.
9.493	2.7080	2.5589	.149	.058275
9.513	2.5110	2.5616	- .051	-.019738
11.710	3.0290	2.8010	.228	.081400
11.710	3.0370	2.8010	.236	.084256
11.710	2.7610	2.8010	- .040	-.014281
11.710	2.8320	2.8010	.031	.011067
11.710	2.9900	2.8010	.189	.067476
14.070	3.0260	3.0156	.010	.003449
14.100	2.7600	3.0180	- .258	-.085487
17.020	3.1490	3.2316	- .083	-.025560
17.560	3.2600	3.2748	- .015	-.004519
17.560	3.4080	3.2748	.133	.040674
17.560	3.2370	3.2748	- .038	-.011543
17.560	3.2810	3.2748	.006	.001893
17.560	3.3460	3.2748	.071	.021742
17.560	3.1750	3.2748	- .100	-.030475
17.560	3.4220	3.2748	.147	.044949
20.340	3.9270	3.4370	.490	.142566
35.130	4.0890	4.0852	.004	.000930
35.130	4.1630	4.0852	.078	.019044
35.130	4.7000	4.0852	.615	.150494
35.620	4.5010	4.1048	.396	.096521
42.490	4.3560	4.3197	.036	.008408
42.490	4.2790	4.3197	- .041	-.009417
42.490	4.2840	4.3197	- .036	-.008260

TABLE V (Contd)

RELATIVE ERROR DETERMINATIONS FOR POSITIVE DURATION

λ	$\Delta^e t_{+s}$	$\Delta^c t_{+s}$	DIFF.	R. E.
46.730	4.3320	4.4519	- .120	-.026932
46.730	4.2980	4.4519	- .154	-.034570
58.550	4.5530	4.7452	- .192	-.040504
58.550	4.2040	4.7452	- .541	-.114052
81.360	5.4170	5.2004	.217	.041651
81.360	5.1910	5.2004	- .009	-.001808
81.360	5.4170	5.2004	.217	.041651
81.360	5.1910	5.2004	- .009	-.001808
99.000	5.2200	5.4380	- .218	-.040088
116.800	5.8110	5.7020	.109	.019116
116.800	5.7420	5.7020	.040	.007015
153.700	5.6430	6.0870	- .444	-.072942
153.700	6.3190	6.0870	.232	.038114
166.900	5.7070	6.2190	- .512	-.082328
166.900	5.8290	6.2190	- .390	-.062711
199.900	6.0220	6.4793	- .457	-.070579
199.900	6.7560	6.4793	.277	.042705
250.400	6.0900	6.7924	- .702	-.103410
316.400	8.1500	7.1686	.981	.136909
316.400	6.3190	7.1686	- .850	-.118512
428.400	7.6050	7.6437	- .039	-.005066
428.400	8.3430	7.6437	.699	.091484
428.400	8.4340	7.6437	.790	.103389
428.400	8.0550	7.6437	.411	.053806
428.400	8.3430	7.6437	.699	.091484

$\Delta^e t_{+s}$ = DURATION OF EXPERIMENTAL POINT.

$\Delta^c t_{+s}$ = DURATION AS OBTAINED FROM THE STANDARD CURVE AT THE CORRESPONDING LAMDA.

DIFF. = $\Delta^e t_{+s} - \Delta^c t_{+s}$

R. E. = $\dfrac{\text{DIFF.}}{\Delta^c t_{+s}}$

Average Positive Relative Error	0.097
Average Negative Relative Error	0.095
Average Relative Error	0.0006
Average Absolute Relative Error	0.096

The computations indicate that two-thirds of all points fall within plus or minus 9.6 percent of the composite curve. It should be noted that the fit of the data to the individual curves presented in Figures 2 through 4 shows a much smaller scatter than indicated for the composite curve.

Positive Impulse Curves

The development of the positive impulse curves followed the same procedure as described for the positive duration. There were fewer points available for determining positive impulse than there were for duration because in some instances the duration of a pressure-time recording was valid but the peak overpressure was not valid. Therefore, the record could not be used to determine positive impulse. In other instances the rate of decay of pressure behind the shock front was not classical, and here again the record was discarded because the impulse was not considered representative of an undisturbed blast wave.

In Table VI the scaled distances and scaled positive impulses have been listed for the 5-ton TNT shot. These scaled values have been plotted in Figure 7. The curve drawn through the points shows an excellent fit with very little scatter in the scaled values of positive impulse. The shape of the curve over this range of scaled distances lends itself to a least-squares fitting technique. However, this was not done because of the small number of points in the case of the 5-ton analysis.

The scaled positive impulse and distance values listed in Table VII for the 20-ton shot have been plotted in Figure 8. Here again as in Figure 7 there is very little scatter of the points about the curve. Out to a distance of 20λ the positive impulse curve for the 20-ton shot agrees well with the 5-ton shot. At distances greater than this, the two curves separate and the 20-ton curve is lower than the 5-ton curve.

TABLE VI

SCALED POSITIVE IMPULSE AND DISTANCE VALUES FOR
A 5-TON TNT DETONATION

λ	I_s	λ	I_s
FT/LBS$^{1/3}$	PSI-MSEC/LBS$^{1/3}$	FT/LBS$^{1/3}$	PSI-MSEC/LBS$^{1/3}$
4.75	14.47	42.49	2.16
4.75	16.17	42.49	2.17
7.46	10.21	42.49	2.20
7.46	11.58	81.36	1.07
9.49	9.23	81.36	1.12
20.34	4.95	81.36	1.18
35.62	2.55	316.40	.34

FIG. 7 SCALED POSITIVE IMPULSE VS SCALED DISTANCE FOR A 5 TON TNT DETONATION

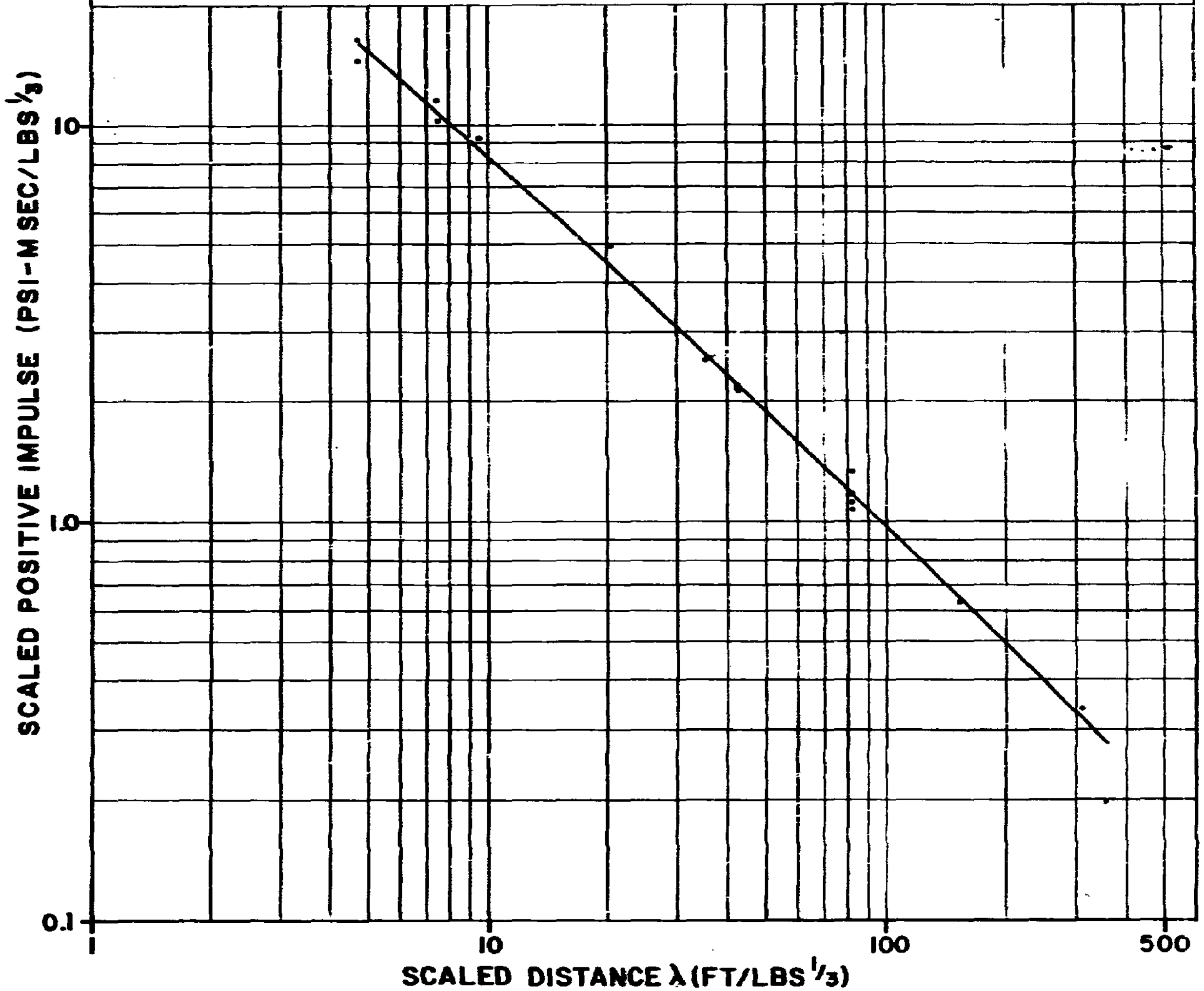

TABLE VII

SCALED POSITIVE IMPULSE AND DISTANCE VALUES FOR A 20-TON TNT DETONATION

λ	I_s	λ	I_s
FT/LBS$^{1/3}$	PSI-MSEC$^{1/3}$	FT/LBS$^{1/3}$	PSI-MSEC/LBS$^{1/3}$
2.34	29.24	11.71	6.89
3.11	20.06	11.71	7.14
3.11	20.68	11.71	7.41
3.11	21.24	17.56	4.04
4.20	18.49	17.56	4.85
4.20	21.83	17.56	4.87
5.77	12.13	17.56	4.87
5.77	12.19	17.56	4.90
5.77	13.26	17.56	4.94
5.77	13.81	17.56	5.09
8.28	9.05	17.56	5.63
8.28	9.05	35.13	2.40
8.28	9.13	35.13	2.44
8.28	9.15	35.13	2.49
8.28	9.63	58.55	1.30
8.28	10.36	58.55	1.35
8.28	10.92	199.90	.42
11.71	6.61	199.90	.43
11.71	6.86	428.40	.18

FIG. 8 SCALED POSITIVE IMPULSE VS SCALED DISTANCE FOR A 20 TON TNT DETONATION

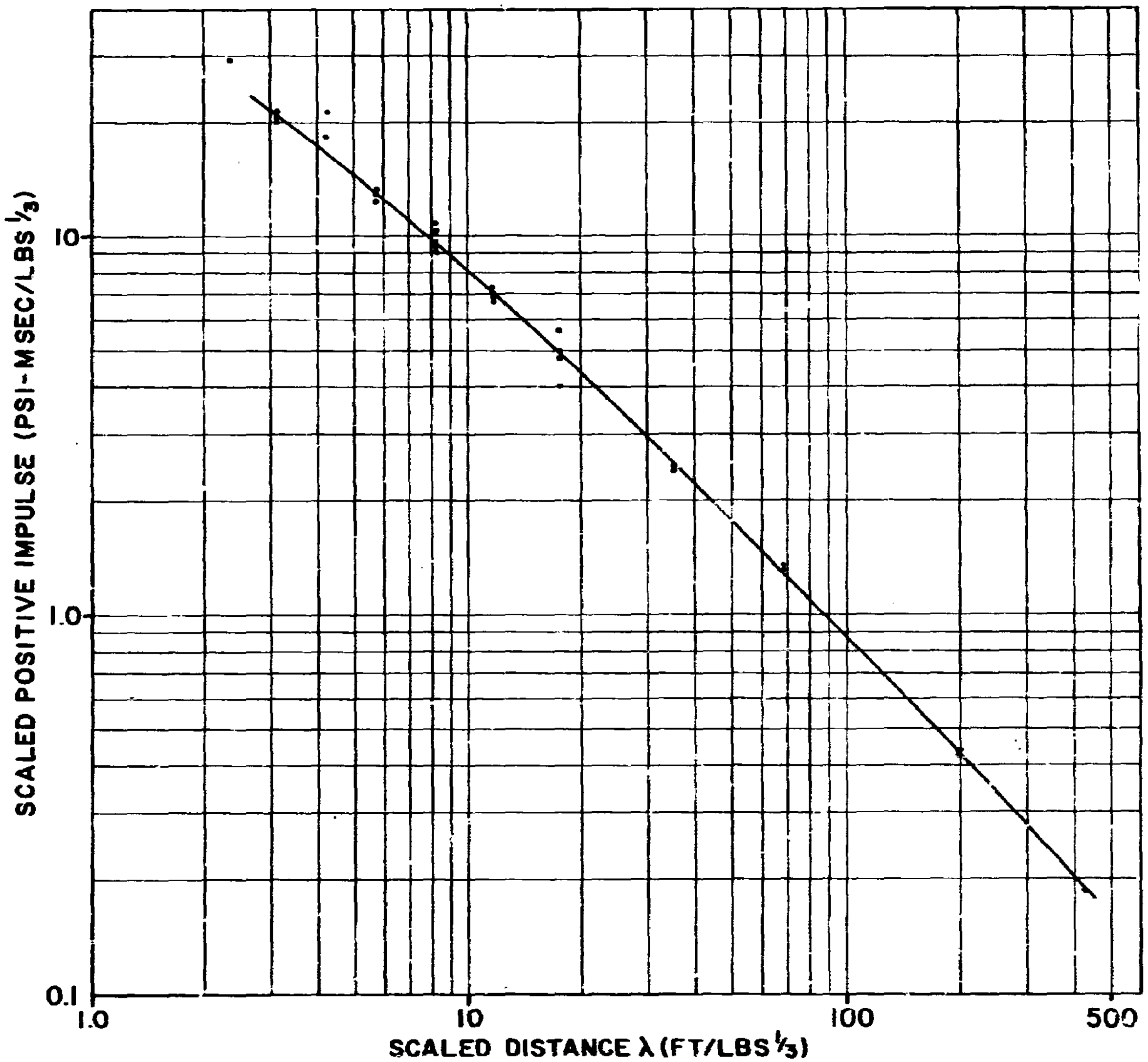

Table VIII contains a listing of the scaled distance and impulse values for the 100-ton shot. These values have been plotted in Figure 9 and a curve drawn to best represent the scaled data. In comparing this curve with the 20-ton curve it can be seen that they tend to coincide at distance greater than 8λ and there is a maximum separation of less than three per cent at 4λ.

The scaled values of distance and positive impulse for the 500-ton shot are listed in Table IX and the same values have been plotted in Figure 10. This report presents for the first time, impulse values at scaled distances of less than 2λ. Records were obtained on the other shots at distances less than 2λ, but they were always considered of very poor quality and unreliable for impulse calculations. When the curve for positive impulse presented in Figure 10 is compared with the 100-ton curve in Figure 9 there is excellent agreement with only a slight separation over the mid-range. Comparison of the 500-ton curve with the 20-ton curve shows a similar trend and here again the agreement is excellent. The comparison between the 500-ton curve and the 5-ton curve presented in Figure 7 shows the same trend as evidenced in the positive duration comparisons. That is, the 5-ton curve is higher than the 500-ton curve. This would be expected since the impulse is a function of positive duration and if the duration is longer then the positive impulse would be expected to be greater, providing the overpressures and decay rate are similar. In Figure 11 all of the data have been plotted and a curve drawn through them. The listing of these values along with values read from the curve at similar λ's is presented in Table X. This table also presents the difference between the experimental values and the "best-fit" curve. From these differences the relative errors were calculated along with other pertinent information relative to how well the curve represents the data.

TABLE VIII

SCALED POSITIVE IMPULSE AND DISTANCE VALUES FOR A 100-TON TNT DETONATION

λ	I_s	λ	I_s
FT/LBS$^{1/3}$	PSI-MSEC/LBS$^{1/3}$	FT/LBS$^{1/3}$	PSI-MSEC/LBS$^{1/3}$
4.36	18.97	7.76	9.58
4.99	14.72	8.76	8.70
5.02	13.38	9.51	8.82
5.57	12.01	14.07	5.84
5.57	15.30	17.02	4.96
5.84	12.25	46.73	1.83
6.11	12.31	46.73	1.73
6.84	11.93	116.80	.71
6.89	12.53	166.90	.46
7.39	10.27	166.90	.51
7.39	10.47	250.40	.29

FIG.9 SCALED POSITIVE IMPULSE VS SCALED DISTANCE FOR A 100 TON TNT DETONATION

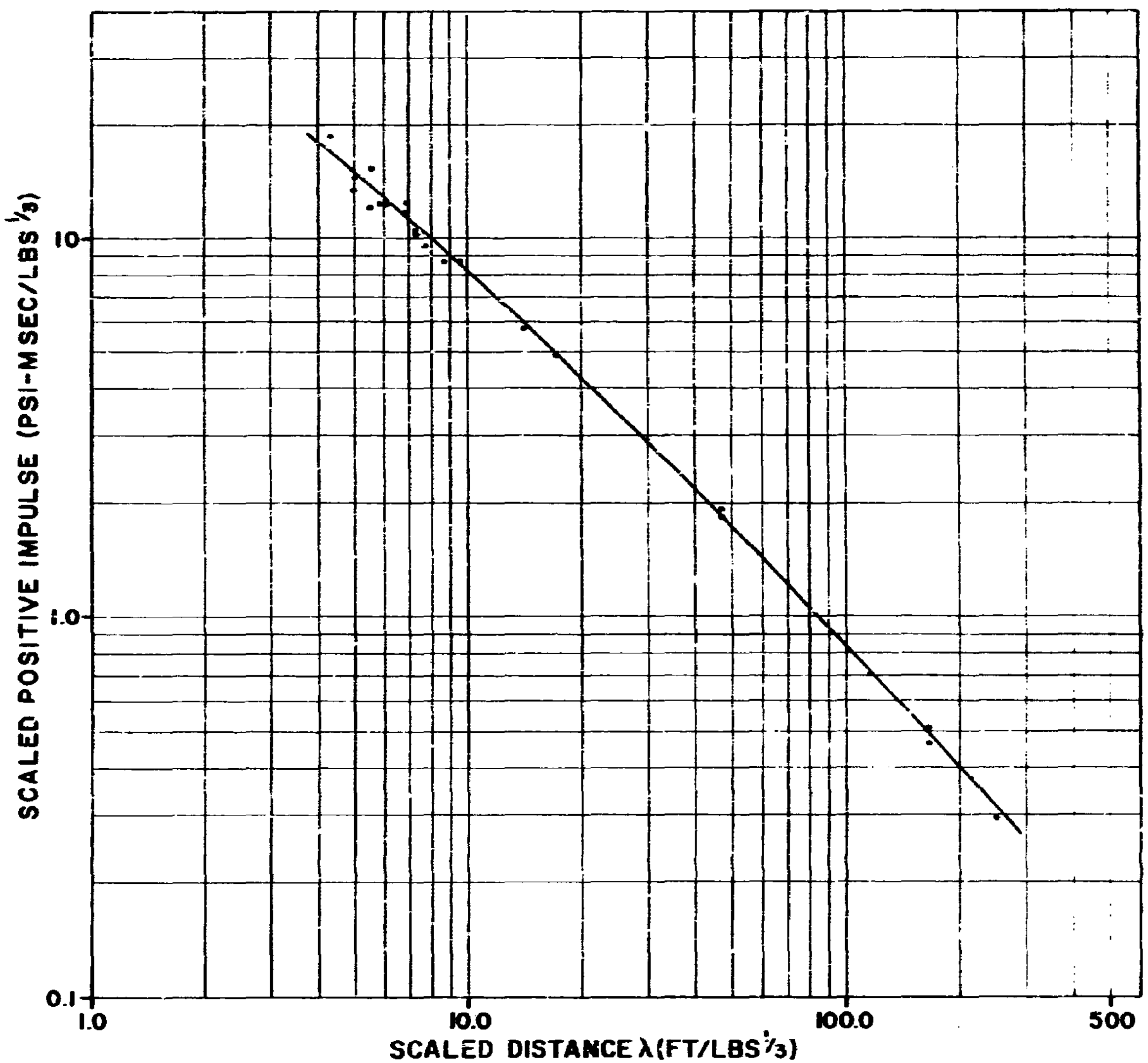

TABLE IX

SCALED POSITIVE IMPULSE AND DISTANCE VALUES FOR
A 500-TON TNT DETONATION

λ	I_s	λ	I_s
FT/LBS$^{1/3}$	PSI-MSEC/LBS$^{1/3}$	FT/LBS$^{1/3}$	PSI-MSEC/LBS$^{1/3}$
.49	44.60	6.13	10.30
.79	24.00	6.72	11.20
1.71	19.30	7.80	9.01
2.97	27.20	7.80	10.00
2.97	28.40	7.80	10.50
3.46	21.30	9.35	8.14
3.46	23.90	9.35	8.85
4.14	14.30	14.10	5.42
4.53	15.20	37.90	2.30
5.55	11.30	99.00	.95
5.55	13.40	250.40	.29

FIG. 10 SCALED POSITIVE IMPULSE VS SCALED DISTANCE
FOR A 500 TON TNT DETONATION

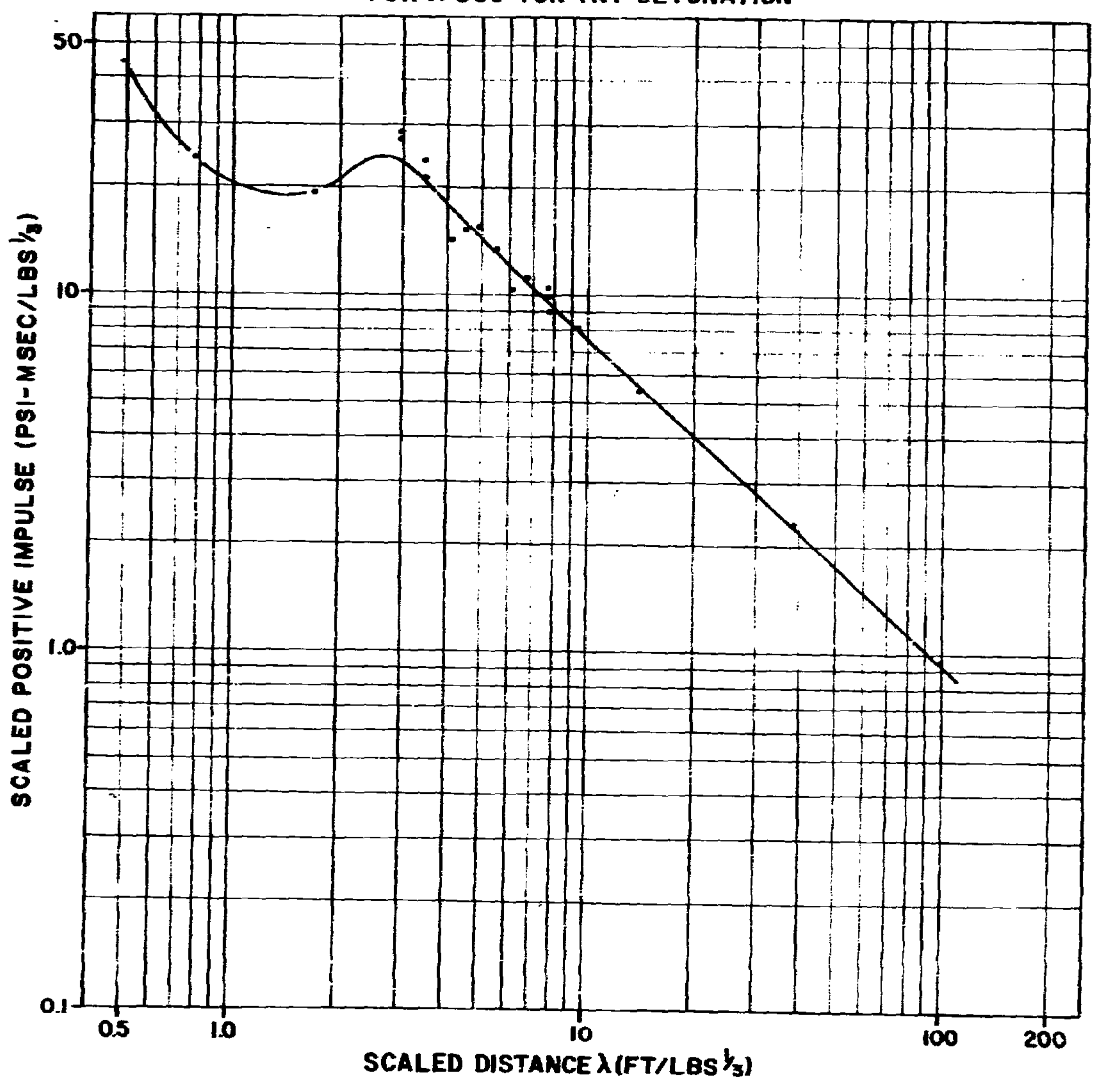

TABLE X

RELATIVE ERROR DETERMINATION FOR POSITIVE IMPULSE

λ	$^{e}I_{s}$	$^{c}I_{s}$	DIFF.	R. E.
.487	44.6000	44.8000	- .200	-.004464
.789	24.0000	23.6300	.370	.015658
1.710	19.3000	19.2800	.020	.001037
2.342	29.2400	25.8040	3.436	.133158
2.970	27.2000	24.0800	3.120	.129568
2.970	28.4000	24.0800	4.320	.179402
3.113	20.6800	23.2220	-2.542	-.109465
3.113	20.0600	23.2220	-3.162	-.136164
3.113	21.2400	23.2220	-1.982	-.085350
3.460	23.9000	21.3080	2.592	.121644
3.460	21.3000	21.3080	- .008	-.000375
4.140	14.3000	17.9680	-3.668	-.204141
4.198	21.8300	17.7476	4.082	.230025
4.198	18.4900	17.7476	.742	.041831
4.356	18.9700	17.1472	1.823	.106303
4.530	15.2000	16.5100	-1.310	-.079346
4.746	14.4700	15.8620	-1.392	-.087757
4.746	16.1700	15.8620	.308	.019417
4.990	14.7200	15.1300	- .410	-.027098
5.024	13.3200	15.0376	-1.718	-.114220
5.550	13.4000	13.7000	- .300	-.021898
5.550	11.3000	13.7000	-2.400	-.175182
5.574	15.3000	13.6520	1.648	.120715
5.574	12.0100	13.6520	-1.642	-.120275
5.769	13.2600	13.2620	- .002	-.000151
5.769	12.1900	13.2620	-1.072	-.080832
5.769	12.1300	13.2620	-1.132	-.085357
5.769	13.8100	13.2620	.548	.041321
5.841	12.2500	13.1180	- .868	-.066169
6.109	12.3100	12.6038	- .294	-.023310
6.130	10.3000	12.5660	-2.266	-.180328
6.720	11.2000	11.5480	- .348	-.030135
6.843	11.9300	11.3512	.579	.050990
6.893	12.5300	11.2712	1.259	.111683
7.394	10.4700	10.5484	- .078	-.007432
7.394	10.2700	10.5484	- .278	-.026393
7.459	10.2100	10.4574	- .247	-.023658
7.459	11.5800	10.4574	1.123	.107350
7.761	9.5810	10.1129	- .532	-.052596
7.800	9.0100	10.0700	-1.060	-.105263
7.800	10.5000	10.0700	.430	.042701
7.800	10.0000	10.0700	- .070	-.006951
8.282	10.3600	9.5680	.792	.082776
8.282	9.1320	9.5680	- .436	-.045569
8.282	9.0520	9.5680	- .516	-.053930
8.282	10.9200	9.5680	1.352	.141304
8.282	9.6290	9.5680	.061	.006375

TABLE X (Contd)

RELATIVE ERROR DETERMINATION FOR POSITIVE IMPULSE

λ	$^{e}I_{s}$	$^{c}I_{s}$	DIFF.	R. E.
8.282	9.1480	9.5680	- .420	-.043896
8.282	9.0460	9.5680	- .522	-.054557
8.762	8.6980	9.1142	- .416	-.045665
9.350	8.1400	8.5850	- .445	-.051835
9.350	8.8500	8.5850	.265	.03[illegible]868
9.493	9.2300	8.4563	.774	.091494
9.513	8.8210	8.4409	.380	.045[illegible]31
11.710	7.1360	7.0240	.112	.015945
11.710	7.4070	7.0240	.383	.054527
11.710	6.8870	7.0240	- .137	-.019505
11.710	6.6070	7.0240	- .417	-.059368
11.710	6.8650	7.0240	- .159	-.022637
14.070	5.8430	5.9755	- .132	-.022174
14.100	5.4200	5.9650	- .545	-.091366
17.020	4.9570	4.9954	- .038	-.007687
17.560	4.0370	4.8712	- .834	-.171251
17.560	4.9390	4.8712	.068	.013919
17.560	5.0890	4.8712	.218	.044712
17.560	4.8750	4.8712	.004	.000780
17.560	4.8980	4.8712	.027	.005502
17.560	4.8660	4.8712	- .005	-.001067
17.560	4.8470	4.8712	- .024	-.004968
17.560	5.6310	4.8712	.760	.155978
20.340	4.9530	4.2354	.718	.169429
35.130	2.4390	2.5027	- .064	-.025460
35.130	2.3980	2.5027	- .105	-.041842
35.130	2.4870	2.5027	- .016	-.006281
35.620	2.5540	2.4753	.079	.031802
42.490	2.2050	2.0955	.110	.052275
42.490	2.1560	2.0955	.061	.028891
42.490	2.1710	2.0955	.076	.036049
46.730	1.8330	1.9143	- .081	-.042459
46.730	1.9270	1.9143	.013	.006655
58.550	1.3520	1.5306	- .179	-.116686
58.550	1.3010	1.5306	- .230	-.150007
81.360	1.1220	1.1037	.018	.016599
81.360	1.1800	1.1037	.076	.069150
81.360	1.0730	1.1037	- .031	-.027798
99.000	.9500	.8140	.136	.167064
116.800	.7052	.7574	- .052	-.068920
166.900	.4639	.5077	- .044	-.086260
166.900	.5144	.5077	.007	.013210
199.900	.4209	.4250	- .004	-.009677
199.900	.4336	.4250	.009	.020204
250.400	.2918	.3221	- .030	-.094095
316.400	.3399	.2526	.087	.345557
428.400	.1849	.1879	- .003	-.016154

FIG.11 COMPOSITE SCALED POSITIVE IMPULSE VS SCALED DISTANCE FOR 5,20,100 AND 500 TON TNT DETONATIONS

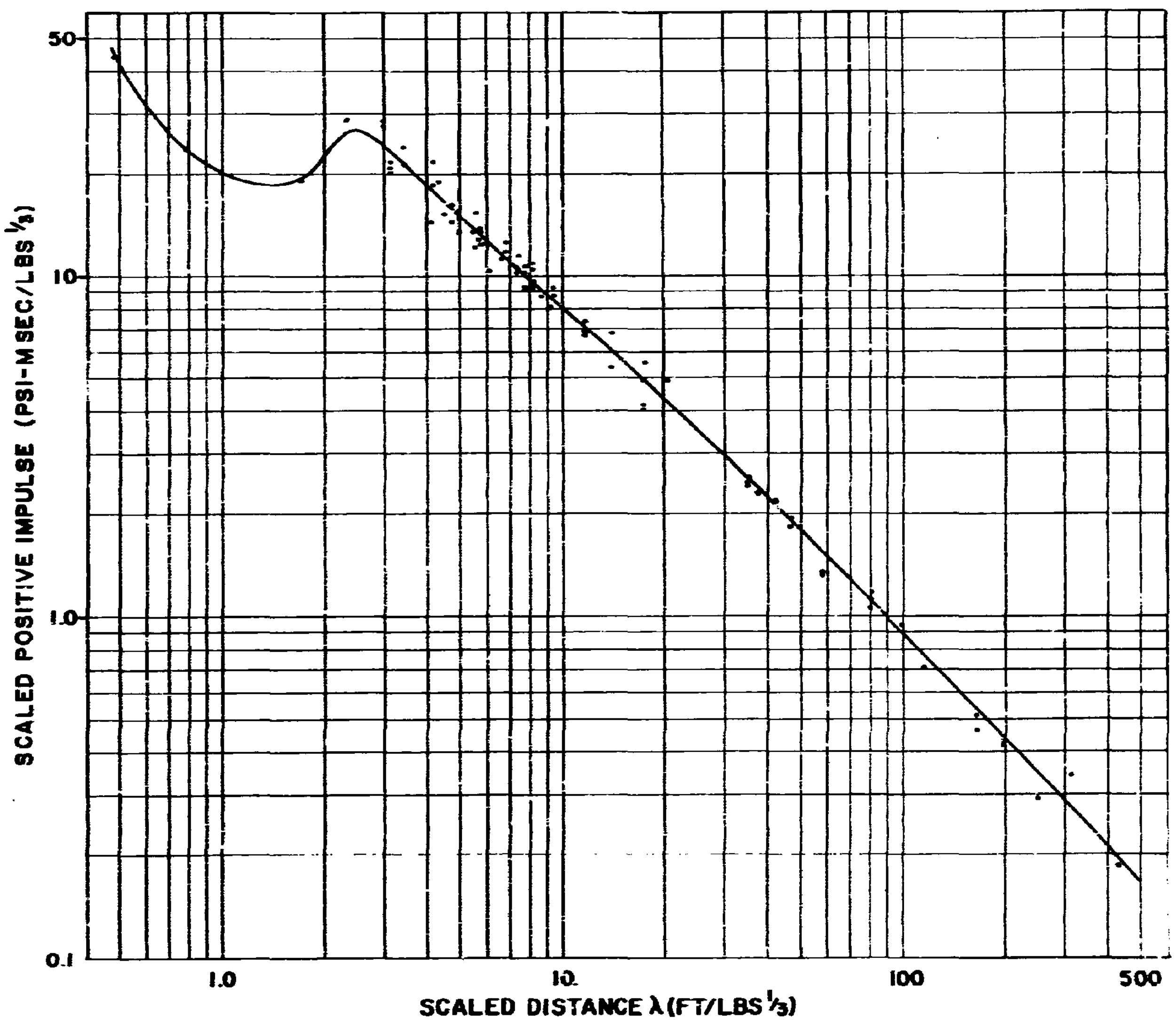

Some of these values are presented below:

Number of Positive Points	41
Number of Negative Points	53
Total Number of Points	94
Average Positive Relative Error	0.076
Average Negative Relative Error	-0.061
Average Relative Error	-0.0014
Average Absolute Relative Error	0.067

There are 12 more values below the curve than above, and approximately two-thirds of the points below the curve fall within 6 percent of the curve and two-thirds of the points above the curve fall within 7.6 percent. Approximately two-thirds of all data points fall within plus or minus 6.7 percent of the curve. This value indicates a better fit or less scatter in the data when compared with the 9.6 percent figure from the positive duration analysis.

Arrival Time Curves

This report considers many hundreds of measurements of arrival time at various radial distances from ground zero recorded on the series of four shots. The values used are primarily those recorded by the various electronic pressure transducers.

The first set of values are presented in Table XI. These are scaled distances and arrival time values for the 5-ton shot and they are plotted in Figure 12. A curve has been drawn through the points and shows very little scatter about the curve. The arrival times measured by the pressure transducers show excellent agreement with arrival times obtained from the photo-optical method used by the Canadians.

In Table XII the scaled distances and arrival times for the 20-ton shot are listed. There was tripartite participation on this shot and the United Kingdom and Canada also made blast measurements. The measurements recorded by the U.S. team show excellent agreement with those of the other two countries, therefore only the U.S. values are

TABLE XI

SCALED ARRIVAL TIME AND DISTANCE VALUES FOR
A 5-TON TNT DETONATION

λ	t_{as}	λ	t_{as}
FT/LBS$^{1/3}$	MSEC/LBS$^{1/3}$	FT/LBS$^{1/3}$	MSEC/LBS$^{1/3}$
1.49	.14	9.49	4.15
1.72	.18	20.34	13.27
2.26	.27	35.62	26.09
3.16	.54	42.49	32.05
4.75	1.17	81.36	66.31
6.01	1.85	153.70	131.10
7.46	2.75	316.40	272.10

FIG. 12 SCALED DISTANCE VS SCALED ARRIVAL TIME
FOR A 5 TON TNT DETONATION

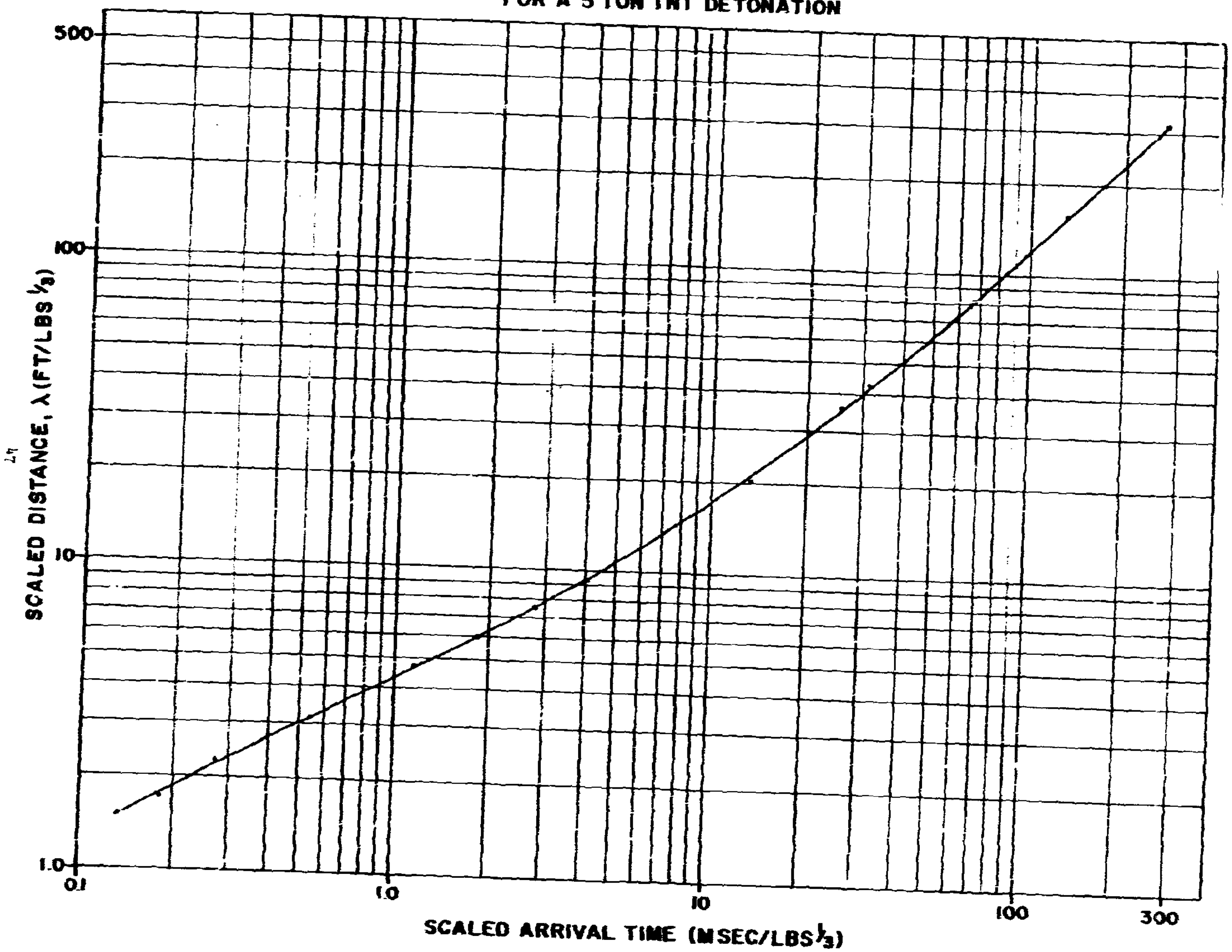

TABLE XII

SCALED ARRIVAL TIME AND DISTANCE VALUES FOR
A 20-TON TNT DETONATION

λ	t_{as}	λ	t_{as}
FT/LBS$^{1/3}$	MSEC/LBS$^{1/3}$	FT/LBS$^{1/3}$	MSEC/LBS$^{1/3}$
1.14	.09	8.28	3.21
1.28	.12	11.71	5.76
1.57	.16	17.56	10.45
2.34	.31	35.13	25.63
3.11	.52	58.55	46.64
4.20	.90	199.90	169.10
5.77	1.65		

FIG. 13 SCALED DISTANCE VS SCALED ARRIVAL TIME
FOR A 20 TON TNT DETONATION

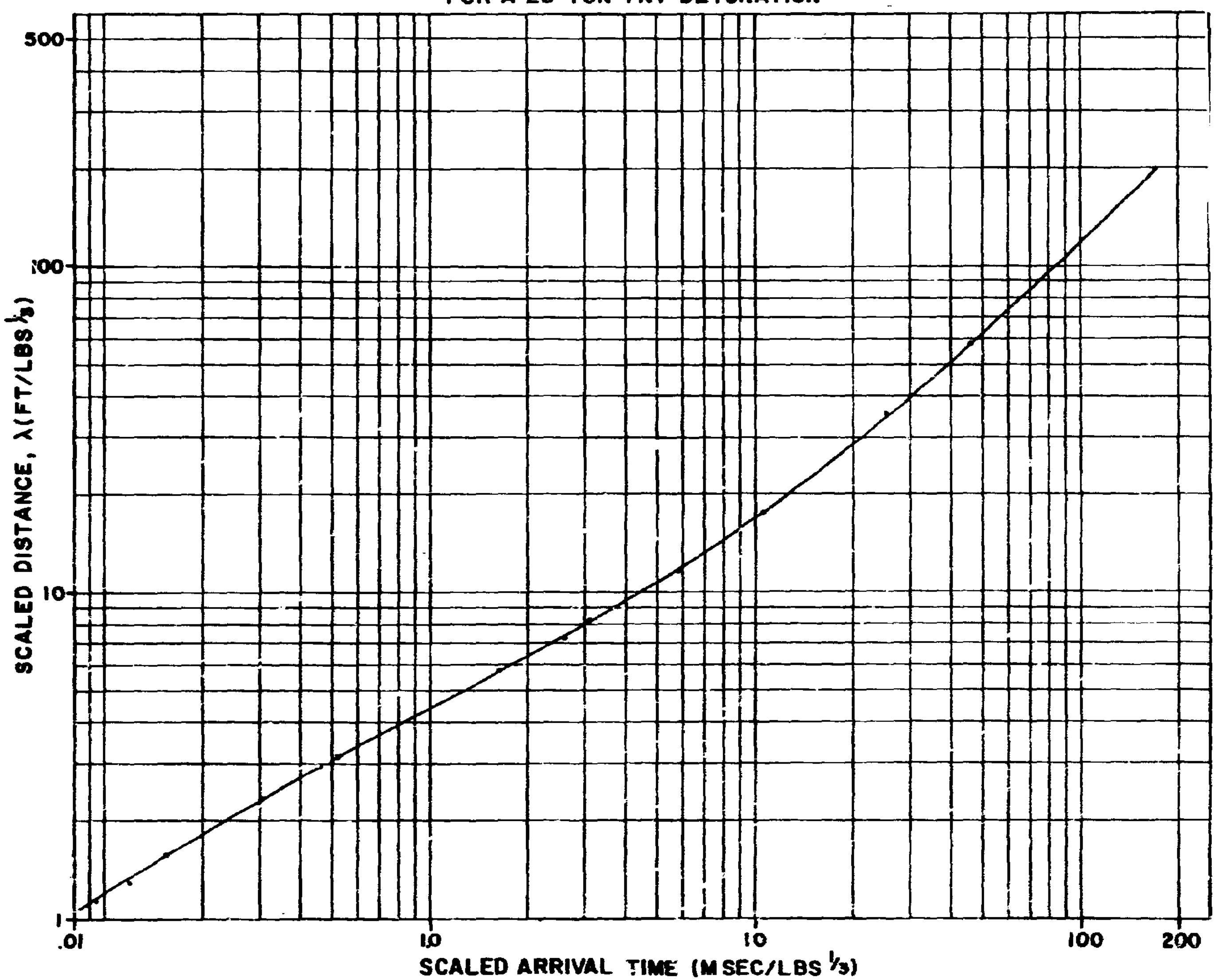

presented in Table XII. A comparison of the scaled arrival time versus distance curve for the 5-ton shot presented in Figure 12 and the curve for the 20-ton shot presented in Figure 13 show excellent agreement.

The scaled values of distance and arrival time for the 100-ton shot are listed in Table XIII and shown plotted in Figure 14. They show excellent agreement with measurements made by the other two participating countries. The curve drawn through the points in Figure 14 also shows excellent agreement with the curve constructed for the 20-ton values plotted in Figure 13. From the analysis of the curves for the 5-, 20-, and 100-ton scaled arrival time values, cube-root scaling is validated for this parameter. There does not seem to be any trend evident as shown on the positive duration or positive impulse.

On the 500-ton TNT shot there were hundreds of measurements made of the arrival time of the shock front at various radial distances from ground zero. The arrival times recorded by BRL along the basic blast line will be used in this report plus some close-in measurements made by the Sandia Corporation (SC) using the slifer cable technique.[5] The scaled arrival times and distances for the 500-ton shot are listed in Table XIV for the BRL measurements, and Table XV contains the close-in slifer-cable data. These data are plotted in Figure 15 with a curve drawn to indicate a best fit as determined by a visual inspection.

A composite curve, Figure 16, was constructed from the scaled values presented in Tables XI through XV. The analysis of the scaled data and values from the composite curve at similar scaled distances is presented in Table XVI. The overall agreement of the scaled arrival time data over the range of 5- to 500-tons is excellent. It can be concluded that cube-root scaling has been validated for arrival time over this

TABLE XIII

SCALED ARRIVAL TIME AND DISTANCE VALUES FOR
A 100-TON TNT DETONATION

λ	t_{as}	λ	t_{as}
$FT/LBS^{1/3}$	$MSEC/LBS^{1/3}$	$FT/LBS^{1/3}$	$MSEC/LBS^{1/3}$
2.34	.35	6.89	2.34
3.40	.64	7.39	2.58
3.87	.78	7.76	2.78
4.36	1.00	8.76	3.56
4.66	1.12	9.51	4.04
4.99	1.27	14.07	7.69
5.02	1.32	17.02	10.09
5.57	1.55	46.73	36.54
5.84	1.75	116.80	99.17
6.11	1.79	166.80	144.40
6.84	2.34	250.40	217.50

FIG. 14 SCALED DISTANCE VS SCALED ARRIVAL TIME FOR A 100 TON TNT DETONATION

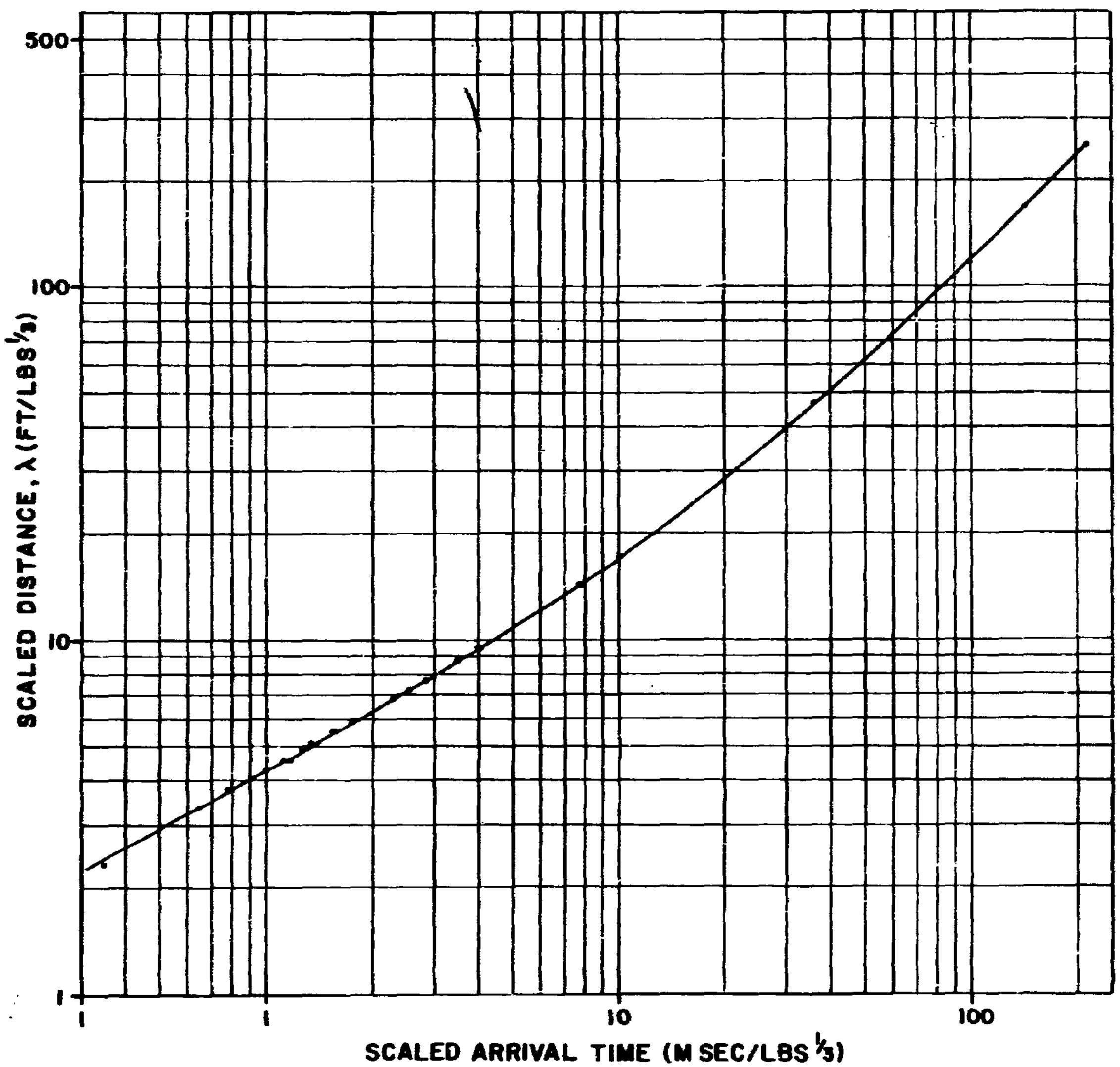

TABLE XIV

SCALED ARRIVAL TIME AND DISTANCE VALUES (BRL) FOR
A 500-TON TNT DETONATION

λ	t_{as}	λ	t_{as}
FT/LBS$^{1/3}$	MSEC/LBS$^{1/3}$	FT/LBS$^{1/3}$	MSEC/LBS$^{1/3}$
.49	.03	4.53	1.10
.79	.05	4.97	1.29
1.03	.09	5.55	1.61
1.71	.19	6.72	2.23
2.44	.34	7.80	2.94
2.97	.50	9.35	4.00
3.46	.65		

TABLE XV

SCALED ARRIVAL TIME AND DISTANCE VALUES (SC) FOR A 500-TON TNT DETONATION

λ	t_{as}	λ	t_{as}
FT/LBS$^{1/3}$	MSEC/LBS$^{1/3}$	FT/LBS$^{1/3}$	MSEC/LBS$^{1/3}$
.208	.010	.521	.030
.265	.013	.546	.033
.313	.015	.578	.035
.355	.018	.633	.040
.393	.020	.681	.045
.428	.023	.738	.050
.467	.025	.840	.060
.492	.028	.927	.070

FIG. 15 SCALED DISTANCE VS SCALED ARRIVAL TIME FOR A 500 TON TNT DETONATION

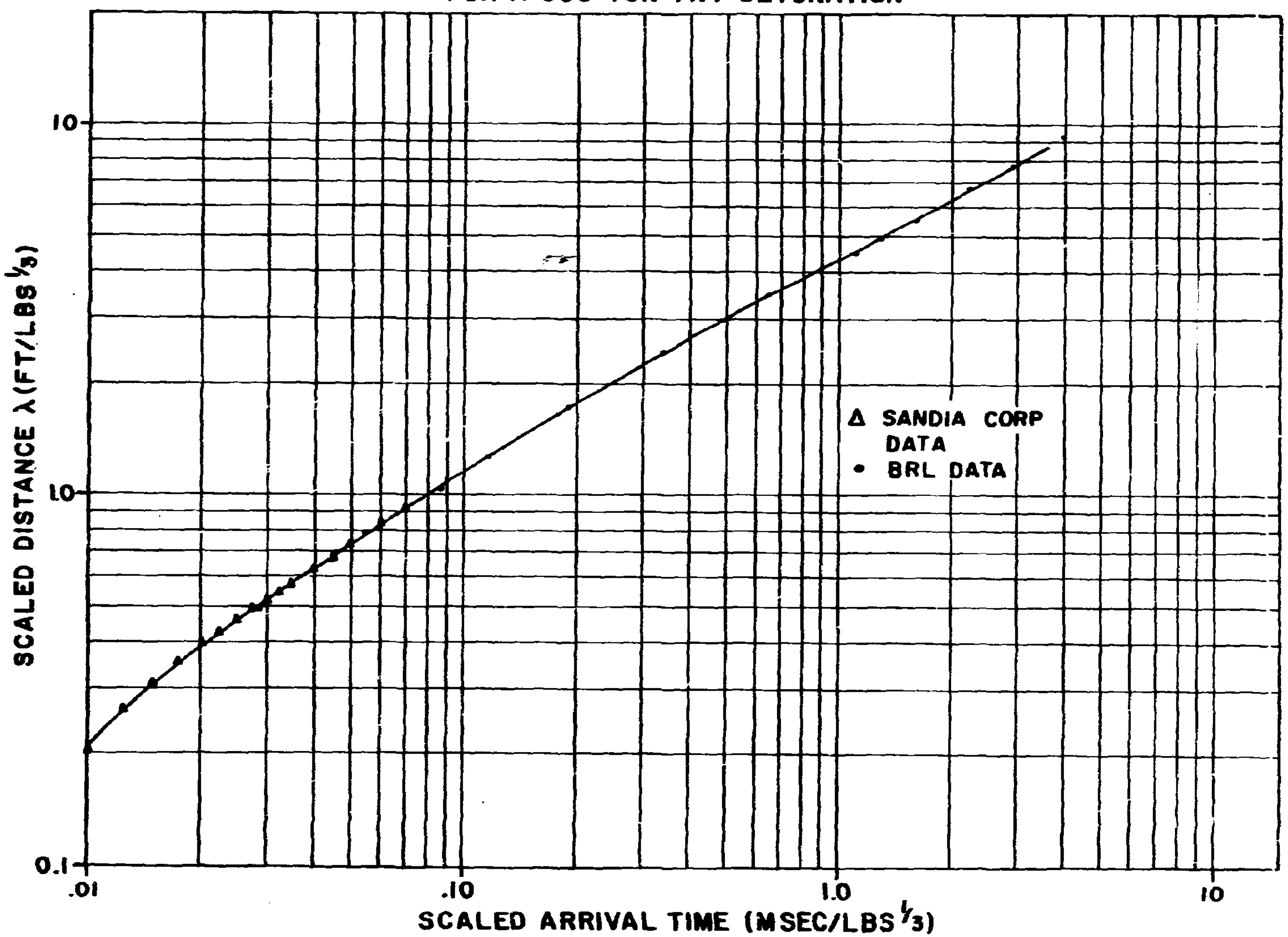

FIG. 16 COMPOSITE CURVE OF SCALED DISTANCE VS SCALED ARRIVAL TIME FOR 5, 20, 100 AND 500 TON TNT DETONATIONS

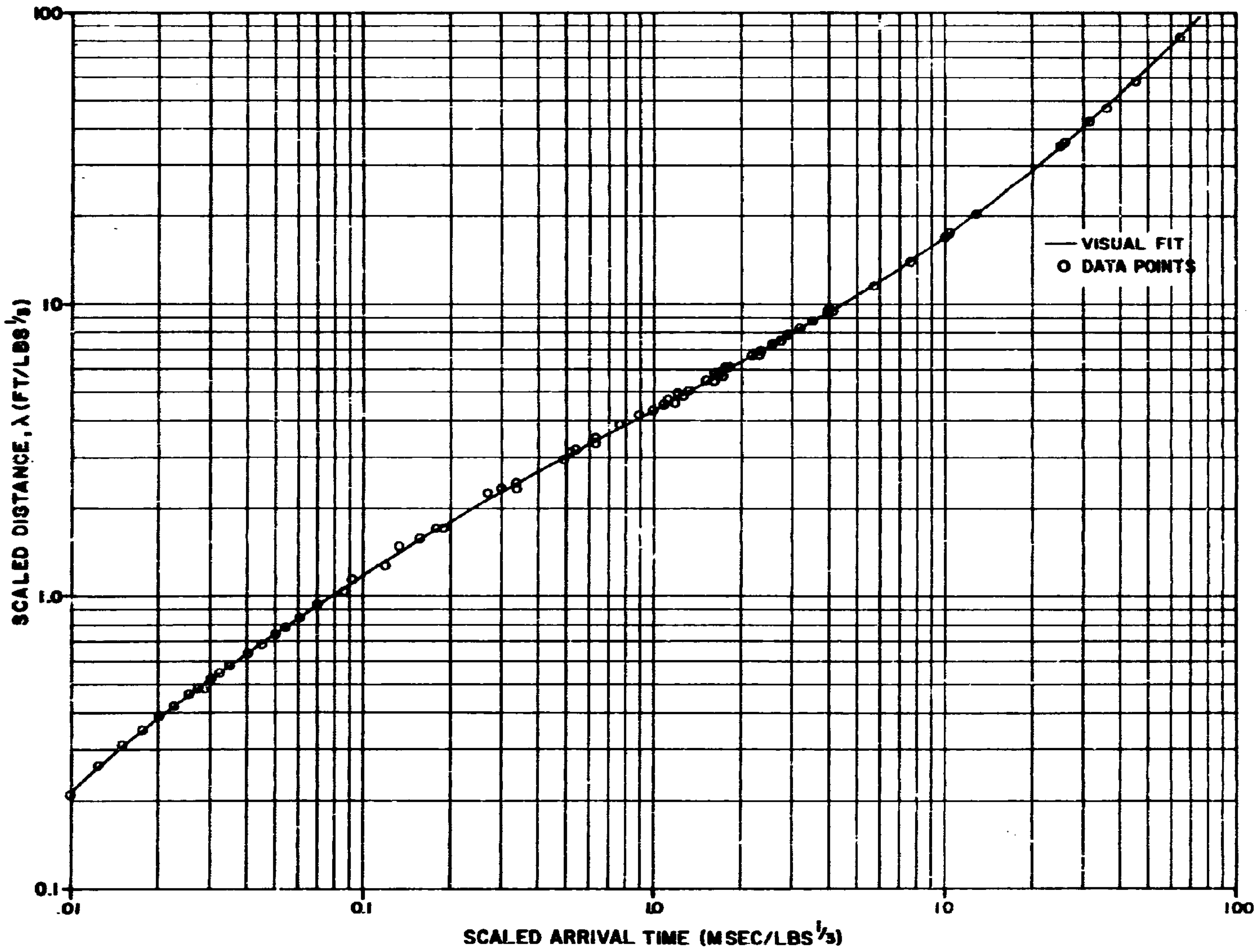

TABLE XVI

RELATIVE ERROR DETERMINATIONS FOR ARRIVAL TIME

λ	et_{as}	ct_{as}	DIFF	R. E.
.208	.0100	.0101	.000	-.003262
.265	.0126	.0126	.000	-.005857
.313	.0151	.0151	.000	-.001458
.355	.0176	.0175	.000	.003058
.393	.0201	.0201	.000	-.002027
.428	.0226	.0226	.000	.001152
.467	.0251	.0255	.000	-.015078
.487	.0285	.0272	.001	.047486
.492	.0276	.0276	.000	-.000897
.521	.0301	.0301	.000	.001083
.546	.0326	.0323	.000	.010867
.578	.0352	.0352	.000	.000114
.633	.0402	.0400	.000	.004842
.681	.0452	.0446	.001	.014135
.738	.0502	.0503	.000	-.002186
.789	.0546	.0551	.000	-.008859
.840	.0603	.0607	.000	-.007362
.927	.0703	.0701	.000	.002870
1.030	.0865	.0821	.004	.053337
1.142	.0940	.0959	- .002	-.020058
1.285	.1204	.1149	.006	.047868
1.492	.1354	.1467	- .011	-.077154
1.571	.1586	.1601	- .001	-.009183
1.710	.1910	.1838	.007	.039173
1.718	.1806	.1852	- .005	-.025049
2.260	.2708	.2991	- .028	-.094617
2.337	.3480	.3172	.031	.097117
2.342	.3055	.3184	- .013	-.040425
2.440	.3400	.3430	- .003	-.008746
2.970	.5000	.4930	.007	.014199
3.113	.5179	.5386	- .021	-.038454
3.164	.5417	.5551	- .013	-.024203
3.405	.6385	.6357	.003	.004405
3.460	.6490	.6544	- .005	-.008252
3.872	.7830	.8123	- .029	-.036028
4.198	.9018	.9462	- .044	-.046904
4.356	1.0000	1.0110	- .011	-.010841
4.530	1.1000	1.0844	.016	.014386
4.657	1.1190	1.1454	- .026	-.023015

TABLE XVI (Contd)

RELATIVE ERROR DETERMINATIONS FOR ARRIVAL TIME

λ	et_{as}	ct_{as}	DIFF	R. E.
4.746	1.1740	1.1881	- .014	-.011851
4.970	1.2900	1.2956	- .006	-.004322
4.990	1.2750	1.3052	- .030	-.023138
5.024	1.3190	1.3210	- .002	-.001544
5.550	1.6100	1.5670	.043	.027441
5.574	1.5500	1.5800	- .030	-.018963
5.769	1.6480	1.6853	- .037	-.022109
5.841	1.7500	1.7241	.026	.014999
6.012	1.8510	1.8165	.035	.019004
6.109	1.7920	1.8689	- .077	-.041127
6.720	2.2300	2.2164	.014	.006136
6.843	2.3450	2.2927	.052	.022829
6.893	2.3380	2.3237	.014	.006171
7.394	2.5790	2.6343	- .055	-.020985
7.459	2.7540	2.6746	.079	.029694
7.761	2.7840	2.8670	- .083	-.028964
7.800	2.9400	2.8920	.048	.016598
8.282	3.2140	3.2118	.002	.000697
8.762	3.5560	3.5539	.002	.000597
9.350	4.0000	3.9750	.025	.006289
9.493	4.1530	4.0751	.078	.019116
9.513	4.0370	4.0896	- .053	-.012867
11.710	5.7610	5.7680	- .007	-.001214
14.070	7.6900	7.6595	.031	.003982
17.020	10.0900	10.2180	- .128	-.012527
17.560	10.4500	10.7040	- .254	-.023729
20.340	13.2700	13.0720	.198	.015147
35.130	25.6300	25.6196	.010	.000406
35.620	26.0900	26.0704	.020	.000752
42.490	32.0500	32.0920	- .042	-.001309
46.730	36.5400	35.6224	.918	.025759
58.550	46.6400	45.7820	.858	.018741
81.360	66.3100	65.4968	.813	.012416
116.800	99.1700	96.7160	2.454	.025373
153.700	131.1000	129.3300	1.770	.013686
166.800	144.4000	140.4400	3.960	.028197
199.900	169.1000	169.9100	- .810	-.004767
250.400	217.5000	215.3200	2.180	.010124
316.400	272.1000	271.7760	.324	.001192

range of yields. Some of the pertinent values obtained from Table XVI are listed below:

Number of Positive Points	40
Number of Negative Points	38
Total Number of Points	78
Average Positive Relative Error	0.0170
Average Negative Relative Error	0.0195
Average Relative Error	0.0007
Average Absolute Relative Error	0.0182

These values show excellent correlation in the number of positive and negative values. The average relative errors are very near the same. Approximately two thirds of the points fall within plus or minus 1.8 percent of the composite curve. The curve shown in Figure 16 presents all data listed in Table XVI except the last six values. For λ's greater than 100 refer to Figure 18.

Peak Overpressure Curve

The peak overpressures measured on the 5-, 20-, and 100-ton TNT shots have been presented in Reference 1. The measurements made in the high overpressure region on the 500-ton shot were more reliable and showed greater consistency then those obtained on any of the preceding shots. The peak overpressure measurements in the close-in region on the 5-, 20-, and 100-ton shots were determined primarily from arrival time measurements and were not higher than 3,000 psi.

On the 500-ton shot the arrival time measurements were started from the detonation point in the charge. The scaled arrival data derived from measurements made by the U.S. on all four shots is presented in Table XVI. Those values plus all Canadian, United Kingdom and U.S. arrival time measurements from other shots were scaled, and an arrival time versus scaled distance curve was calculated, using the equation.[6]

$$\lambda = C_1 + C_2 T + C_3 \ln (1 + T) + C_4 [\ln(1 + T)]^{1/2} \qquad (4)$$

where λ = scaled distance ($D/w^{1/3}$)

$T = t_{as}$ scaled arrival time

$C_{1,2,3,4}$ = constants determined from equation

The arrival values versus scaled distances from .2λ to 2λ established from this equation are listed in Table XVII. Values out to 10λ have been plotted in Figure 17 and a smooth curve drawn through the points. For comparison the data used to establish the curve have also been plotted to show the validity of the curve. This equation was used primarily to establish reliable peak overpressure values in the high overpressure region.

From Equation (4) an arrival time versus distance relation was found and by integration the velocity of the shock front was determined. Scaled distance, arrival time and velocity of the shock front are presented in Table XVII. The Mach velocity of the shock front was determined from a computer program but is not listed in Table XVII. From the Mach value it is possible to obtain the peak overpressure from Equation (2) or from tables presented in Reference 7. The tables listing Mach values versus pressure from Reference 7 were stored in the computer, and from this a tabulation of peak overpressure versus λ was obtained. These values are listed in Table XVII for values of λ from 0.20 to 2.0. We believe that from Reference 1, values of peak overpressure at λ's greater than 1.8 are valid but a modification of the curve in Reference 1 should be made at λ's less than 1.8. The modified portion of the curve plus the established curve is presented in Figure 18.

SUMMARY AND CONCLUSIONS

The scaled values of peak overpressure, arrival time, positive duration, positive impulse and shock front velocity versus scaled distance (λ) are presented in Table XVIII. The values of the velocity of the shock front as determined in the Appendix are listed in Table A1.

TABLE XVII

PEAK OVERPRESSURE CALCULATIONS

λ		ΔP_s		t_{as}	U	
200		69517370	4	95365817-02	21520957	2
250		55987611	4	11989246-01	19368175	2
300		46237775	4	14697305-01	17644526	2
350		38971453	4	17654940-01	16230252	2
400		33409437	4	20856914-01	15048188	2
450		29043789	4	24298537-01	14045359	2
500		25526425	4	27975316-01	13182109	2
550		22637763	4	31883296-01	12430590	2
600		20219804	4	36018838-01	11769658	2
650		18175224	4	40378668-01	11183287	2
700		16448920	4	44959809-01	10658955	2
750		14966832	4	49759597-01	10186852	2
800		13676542	4	54775631-01	97590934	1
850		12554663	4	60005755-01	93692690	1
900		11571693	4	65448129-01	90123153	1
950		10704254	4	71101102-01	86839577	1
100	1	99350823	3	76963158-01	83804392	1
125	1	71171089	3	10937417	71475546	1
150	1	53343835	3	14690535	62363142	1
175	1	41257387	3	18956676	55247952	1
200	1	32591507	3	23744857	49466298	1

FIG. 17 COMPARISON OF DATUM POINTS WITH FITTED CURVE

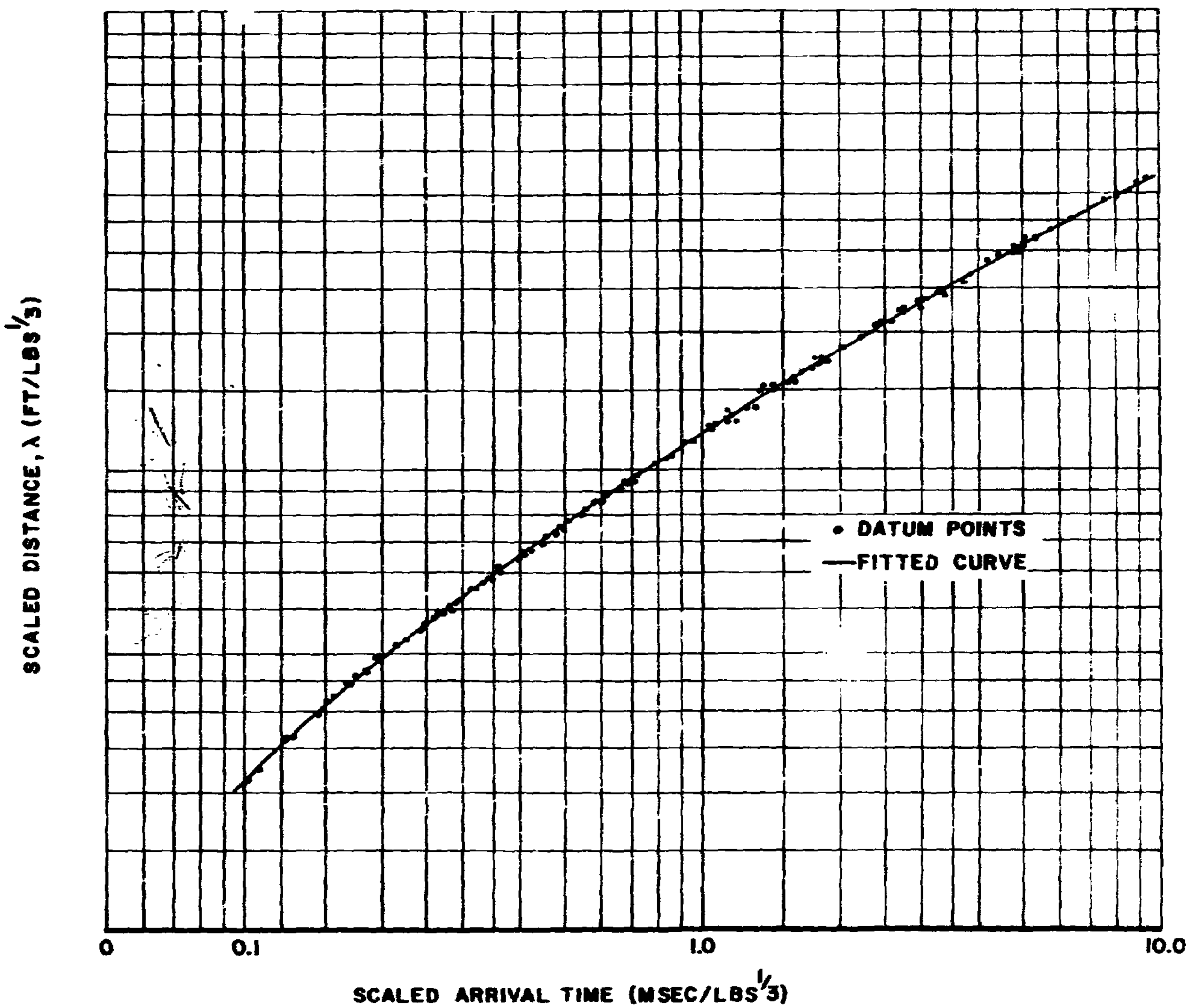

These scaled values of the blast parameters have all been plotted versus scaled distance and presented in Figure 18. The figure may be used as a quick reference for determining the scaled values of the various parameters versus scaled distance as well as their relation to each other.

The accuracy of the curves in relation to the data has been emphasized earlier in this report, but the user is again reminded that the trend noted in the positive duration should be given consideration when predicting the duration to be expected from small yields. The difficulty in recording duration, plus the apparent trend as a function of yield makes the tabulations and associated curve the least accurate of the blast parameters reported here.

The impulse values listed in Table XVIII and the curve presented in Figure 18 are believed to be reasonably accurate in the region greater than 3λ because of the large number of data used. The region less than 3λ may be somewhat questionable because of the scarcity of data in the higher pressure region.

The arrival time values listed in Table XVIII are taken from two sources. (1) The values established from Equation (4) and plotted to 10λ in Figure 17 show good visual agreement with the data points. The equation did not give valid results at λ's greater than 6λ. (That is the peak overpressure calculated from the velocity determinations began to fall lower than the established curve and became negative at 50λ.) (2) The values of λ greater than four, the arrival times were calculated from the peak overpressure versus λ determinations as explained in the Appendix. The arrival time values determined by this method show excellent agreement with the curves presented in Figures 16 and 18. For determining arrival times at less than 4λ, it is recommended that the curve in Figure 17 be used. For arrival times at greater than 4λ, the curve in Figure 18 is recommended. The values in Table XVIII may be used throughout the complete range; the same information is contained in Table A.1 of the Appendix. The arrival time curve in Figure 18 is the same as the composite curve established in Figure 16.

TABLE XVIII

BLAST PARAMETERS VERSUS SCALED DISTANCE

λ FT/LBS$^{1/3}$		ΔP_s PSI		t_{as} MSEC/LBS$^{1/3}$		U FT/MSEC		t_{+s} MSEC/LBS$^{1/3}$		I_s PSI-MSEC/LBS$^{1/3}$	
2000		6952	4	9537-02		21518	2				
2500		5599	4	1199-01		19366	2				
3000		4624	4	1470-01		17645	2				
3500		3897	4	1765-01		16230	2				
4000		3341	4	2086-01		15048	2				
4500		2904	4	2430-01		14046	2	197			
5000		2553	4	2797-01		13182	2	189		422	2
5500		2264	4	3188-01		12431	2	183		363	2
6000		2022	4	3602-01		11770	2	178		321	2
6500		1818	4	4038-01		11183	2	174		290	2
7000		1645	4	4496-01		10659	2	171		267	2
7500		1497	4	4976-01		10187	2	170		248	2
8000		1368	4	5477-01		97591	1	170		233	2
8500		1255	4	6000-01		93692	1	171		223	2
9000		1157	4	6544-01		90123	1	172		214	2
9500		1070	4	7110-01		86840	1	174		207	2
1000	1	9935	3	7696-01		83805	1	178		200	2
1100	1	8602	3	8930-01		78304	1	190		193	2
1200	1	7544	3	1025		73561	1	208		189	2
1300	1	6678	3	1165		69395	1	230		185	2
1400	1	5923	3	1313		65621	1	256		184	2
1500	1	5334	3	1469		62363	1	288		186	2
1600	1	4782	3	1633		59277	1	326		189	2
1700	1	4322	3	1806		56511	1	375		192	2
1800	1	3919	3	1987		53941	1	430		200	2
1900	1	3540	3	2178		51442	1	510		210	2
2000	1	3207	3	2377		49098	1	605		224	2
2200	1	2630	3	2804		44791	1	865		241	2
2400	1	2180	3	3270		41096	1	118	1	265	2
2600	1	1834	3	3777		37982	1	143	1	263	2
2800	1	1558	3	4323		35307	1	159	1	251	2
3000	1	1337	3	4909		32993	1	166	1	239	2
3250	1	1117	3	5698		30509	1	170	1	224	2
3500	1	9438	2	6548		28407	1	170	1	211	2
3750	1	8064	2	7457		26614	1	167	1	198	2
4000	1	6958	2	8426		25073	1	161	1	185	2
4500	1	5316	2	1053	1	22608	1	158	1	166	2
5000	1	4184	2	1284	1	20700	1	157	1	151	2
5500	1	3376	2	1535	1	19236	1	161	1	138	2
6000	1	2782	2	1803	1	18074	1	170	1	128	2
6500	1	2334	2	2087	1	17154	1	183	1	119	2
7000	1	1989	2	2385	1	16409	1	201	1	111	2

TABLE XVIII (Contd)

BLAST PARAMETERS VERSUS SCALED DISTANCE

λ		ΔP_s		t_{as}		U		t_{+s}		I_s	
FT/LBS$^{1/3}$		PSI		MSEC/LBS$^{1/3}$		FT/MSEC		MSEC/LBS$^{1/3}$		PSI-MSEC/LBS$^{1/3}$	
7500	1	1718	2	2696	1	15792	1	216	1	104	2
8000	1	1501	2	3018	1	15290	1	229	1	985	1
8500	1	1323	2	3349	1	14861	1	239	1	935	1
9000	1	1182	2	3690	1	14506	1	248	1	890	1
9500	1	1059	2	4037	1	14199	1	256	1	845	1
1000	2	9615	1	4393	1	13949	1	262	1	810	1
1100	2	8029	1	5121	1	13527	1	273	1	745	1
1200	2	6825	1	5868	1	13201	1	283	1	685	1
1300	2	5920	1	6632	1	12950	1	293	1	645	1
1400	2	5186	1	7408	1	12742	1	301	1	600	1
1500	2	4665	1	8198	1	12589	1	309	1	565	1
1600	2	4177	1	8995	1	12448	1	318	1	535	1
1700	2	3797	1	9801	1	12338	1	323	1	500	1
1800	2	3488	1	1061	2	12247	1	331	1	477	1
1900	2	3208	1	1143	2	12163	1	337	1	452	1
2000	2	2984	1	1226	2	12093	1	342	1	430	1
2200	2	2596	1	1392	2	11975	1	352	1	392	1
2400	2	2299	1	1560	2	11885	1	364	1	362	1
2600	2	2061	1	1728	2	11813	1	372	1	334	1
2800	2	1867	1	1898	2	11755	1	381	1	312	1
3000	2	1706	1	2069	2	11706	1	390	1	293	1
3250	2	1537	1	2283	2	11654	1	399	1	271	1
3500	2	1397	1	2498	2	11610	1	408	1	251	1
3750	2	1279	1	2713	2	11572	1	418	1	237	1
4000	2	1178	1	2930	2	11540	1	424	1	221	1
4500	2	1015	1	3364	2	11488	1	440	1	198	1
5000	2	8876		3800	2	11447	1	455	1	179	1
5500	2	7857		4237	2	11415	1	466	1	163	1
6000	2	7023		4676	2	11388	1	478	1	149	1
6500	2	6328		5115	2	11366	1	487	1	138	1
7000	2	5742		5556	2	11347	1	498	1	128	1
7500	2	5222		5997	2	11331	1	508	1	120	1
8000	2	4769		6438	2	11316	1	518	1	112	1
9000	2	4041		7323	2	11293	1	533	1	945	
1000	3	3484		8209	2	11275	1	545	1	895	
1100	3	3047		9096	2	11261	1	560	1	805	
1200	3	2692		9985	2	11250	1	575	1	735	
1300	3	2405		1087	3	11241	1	585	1	675	
1400	3	2162		1176	3	11233	1	595	1	625	
1500	3	1970		1265	3	11227	1	605	1	585	
1600	3	1793		1355	3	11221	1	615	1	545	
1700	3	1647		1444	3	11217	1	625	1	507	
1800	3	1523		1533	3	11213	1	633	1	480	

TABLE XVIII (Contd)

BLAST PARAMETERS VERSUS SCALED DISTANCE

λ		ΔP_s	t_{as}		U		t_{+s}		I_s
FT/LBS$^{1/3}$		PSI	MSEC/LBS$^{1/3}$		FT/MSEC		MSEC/LBS$^{1/3}$		PSI-MSEC/LBS$^{1/3}$
1900	3	1409	1622	3	11209	1	641	1	451
2000	3	1314	1711	3	11206	1	648	1	425
2200	3	1148	1890	3	11201	1	660	1	383
2400	3	1016	2068	3	11196	1	673	1	351
2600	3	9079-01	2247	3	11193	1	685	1	321
2800	3	8188-01	2426	3	11190	1	697	1	298
3000	3	7430-01	2604	3	11188	1	708	1	275
3250	3	6640-01	2828	3	11185	1	712	1	252
3500	3	5980-01	3051	3	11183	1	735	1	233
3750	3	5430-01	3275	3	11181	1	742	1	217
4000	3	4960-01	3499	3	11180	1	755	1	201
4500	3	4200-01	3946	3	11177	1	772	1	178
5000	3	3620-01	4393	3	11176	1	788	1	
5500	3	3170-01	4841	3	11174	1	803	1	
6000	3	2800-01	5288	3	11173	1	819	1	
6500	3	2500-01	5736	3	11172	1			
7000	3	2260-01	6183	3	11171	1			
7500	3	2050-01	6631	3	11171	1			
8000	3	1870-01	7079	3	11170	1			
9000	3	1580-01	7974	3	11169	1			
1000	4	1370-01	8869	3	11168	1			

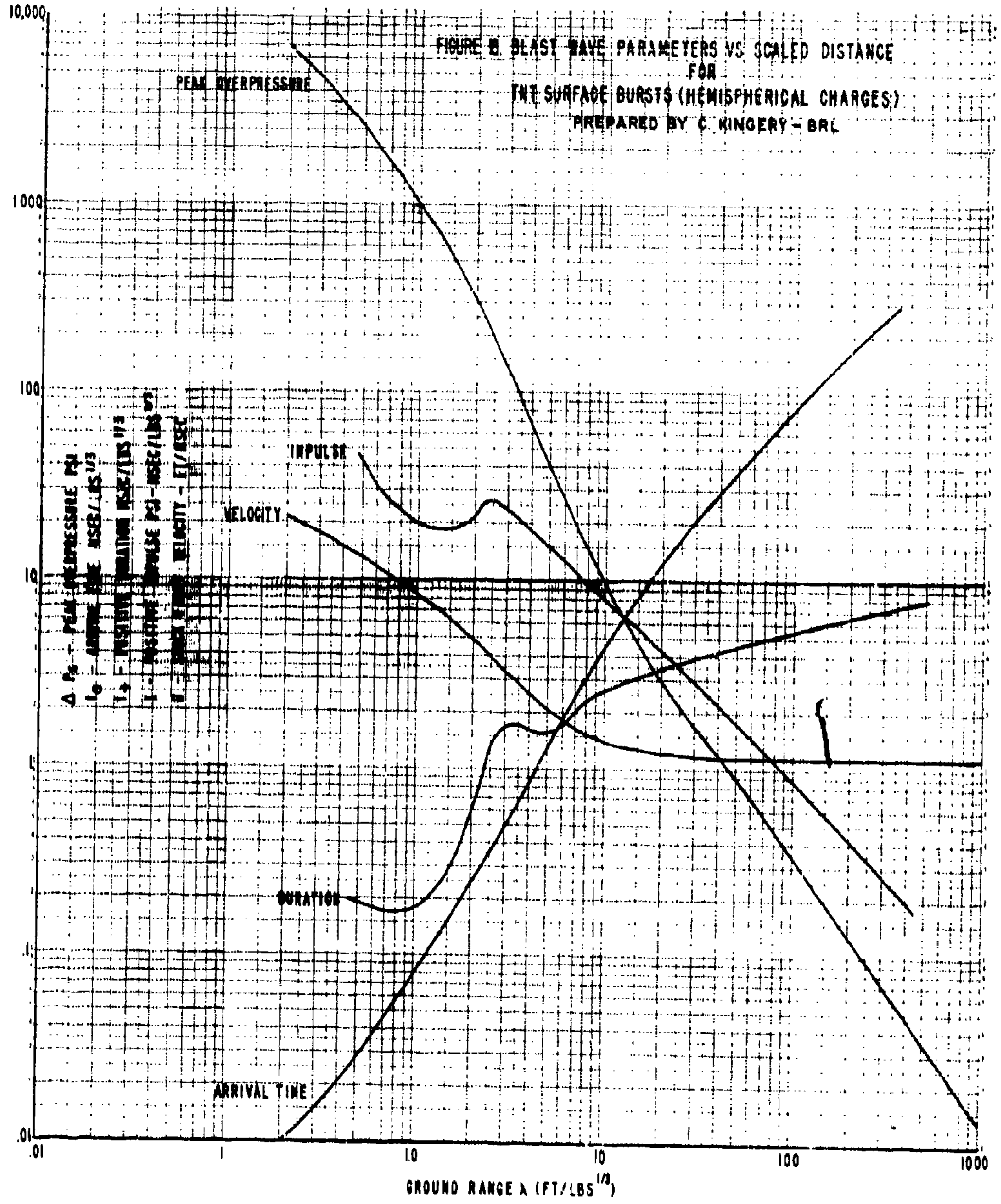
FIGURE 8. BLAST WAVE PARAMETERS VS SCALED DISTANCE
FOR
TNT SURFACE BURSTS (HEMISPHERICAL CHARGES)
PREPARED BY C. KINGERY - BRL
PEAK OVERPRESSURE
IMPULSE
VELOCITY
DURATION
ARRIVAL TIME
10,000
1000
100
10
1
.1
.01
.01
1
1.0
10
100
1000
GROUND RANGE λ (FT/LBS$^{1/3}$)

The peak overpressure values listed in Table XVIII contain the same values established in Reference 1 for λ's greater than 1.8λ. At less than 1.8λ, the peak overpressures were determined from the arrival time measurements. These values are plotted in Figure 18 and are believed to be quite accurate. The peak overpressures listed in Table XVIII were used in the Appendix for calculating the arrival time.

The fifth parameter of general interest is the velocity of the shock front. Values of shock velocity are listed in Table XVIII as a function of λ and were determined in the same way as arrival time. The values from Table XVIII are plotted in Figure 18 and are consistent with both the peak overpressure and arrival time values.

After a thorough analysis of the available data it is quite apparent that information about the duration, impulse and wave shape is lacking for the high overpressure region. This of course implies the need for more measurements of pressure-time with improved instrumentation rather than arrival time measurements. There is also a need for a gage more sensitive to a negative pressure than a positive pressure for determining both the positive and negative durations in the high overpressure region.

ACKNOWLEDGEMENT

The author wishes to acknowledge Wayne Place for his work in the data analysis phase of this report and Buckner F. Pannill for the programming and computer runs.

C. N. KINGERY

REFERENCES

1. Kingery, C. N. and Pannill, B. F. Peak Overpressure Versus Scaled Distance for TNT Surface Bursts (Hemispherical Charges). Ballistic Research Laboratories Memorandum Report No. 1518, April 1964.

2. Kingery, C. N. and others. Preliminary Report-Operation SNOW BALL. Volume 1 and 2, DASA No. 1550-1 and 1550-2, October 1964. (CONFIDENTIAL)

3. Symposium Proceedings: Operation SNOW BALL. Volume 1 and 2, DASA No. 1642-1 (UNCLASSIFIED), DASA No. 1642-2 (SECRET), August 1965.

4. Groves, T. K. Surface Burst 100-ton TNT Hemispherical - Free Field Air Blast Overpressure. Suffield Technical Paper No. 269. Ralston, Canada, October 1962.

5. Chabia, A. J.; Bass, R. C. and Hawk, H. L. Measurements of Wave Fronts in Earth, Air, and Explosive Produced by a 500-Ton Hemisphere of TNT Detonated on the Surface of the Earth. Sandia Corporation Report SC-RR-64-442, November 1965. (OFFICAL USE ONLY)

6. Preliminary Report on the Canadian Projects in the (1964) 500-Ton TNT Suffield Explosion. Suffield Special Publication 45, Fall 1964.

7. Shear, R. E. and Day, B. D. Tables of Thermodynamic and Shock Front Parameters for Air. Ballistic Research Laboratories Memorandum Report No. 1206, May 1959.

PREVIOUS PAGE WAS BLANK, THEREFOR WAS NOT FILMED.

APPENDIX A

INTERNAL CONSISTENCY OF THE ARRIVAL TIME AND PEAK OVERPRESSURE

The shock front velocity of a blast wave is related to the peak overpressure by the Rankine-Hugoniot relationship. Since the velocity of the shock front is equal to the inverse of the derivation of the arrival time curve

$$U = d\lambda/dt_a = {}^{1}/\left(\frac{dt_a}{d\lambda}\right) , \qquad (A1)$$

we can derive the overpressure curve theoretically from the arrival time curve. Employing this procedure it is also possible to test the internal consistency of the experimentally derived curves by comparing them with those derived theoretically.

It has been found that very small variations in arrival time measurements can have extremely adverse effects on the apparent velocity of the shock front and in turn this affects the derived peak overpressure. Therefore, to test the internal consistency of the curve, it was decided to derive a theoretical arrival time curve based on the experimental peak overpressure curve.

In the analysis of the arrival time data it was found that from Equation (4) a good starting point was at distance of λo equal to 0.20 $ft/lb^{1/3}$, where the scaled arrival time t_{as} is 0.00953658 $ms/lb^{1/3}$. The arrival time at any point λ, beyond λo = 0.20 is given by

$$\begin{aligned} t_{as} &= 0.00953658 + \int_{\lambda o = 0.20}^{\lambda} dt_{as} \\ &= 0.00953658 + \int_{\lambda o = 0.20}^{\lambda} \left(\frac{dt_{as}}{d\lambda}\right) d\lambda \qquad (A2) \\ &= 0.00953658 + \int_{\lambda o = 0.20}^{\lambda} \left(\frac{1}{U}\right) d\lambda , \end{aligned}$$

where U equals shock front velocity in ft/ms, t_{as} equals scaled arrival time in $ms/lb^{1/3}$, and λ equals scaled distance from ground zero in $ft/lb^{1/3}$.

The integration was achieved by using the peak overpressure versus scaled distance listed in Table XVIII. Values of scaled horizontal distances were selected as listed with the corresponding peak overpressure. The appropriate value of shock front velocity in Mach units was then selected from the pressure versus Mach values presented in Reference 7. Equation A2 was programmed for the computer and the calculated arrival times are listed in Table A-1, with the peak overpressure, Mach number, velocity, and arrival time.

The curve presenting scaled arrival time versus distance in Figure 18 was obtained from measured values as listed in Table XVI. The values in Table XVI and Table A-1 are different by less than one percent over most of the range, but in trying to use the measured values in the various curve fitting techniques, a lower peak overpressure curve was calculated at the greater distances. In fact the peak overpressure curve calculated showed negative values at λ greater than 100. Therefore, the values listed in Table XVIII and A-1 are recommended for use because they are consistent with a well established peak overpressure curve.

TABLE A-I

ARRIVAL TIME CALCULATIONS

λ		ΔP_s		M		U		t_{as}	
2000		6952	4	19275	2	21518	2	9537-02	
2500		5599	4	17347	2	19366	2	1199-01	
3000		4624	4	15805	2	17645	2	1470-01	
3500		3897	4	14538	2	16230	2	1765-01	
4000		3341	4	13479	2	15048	2	2086-01	
4500		2904	4	12581	2	14046	2	2430-01	
5000		2553	4	11808	2	13182	2	2797-01	
5500		2264	4	11135	2	12431	2	3188-01	
6000		2022	4	10543	2	11770	2	3602-01	
6500		1818	4	10017	2	11183	2	4038-01	
7000		1645	4	95477	1	10659	2	4496-01	
7500		1497	4	91248	1	10187	2	4976-01	
8000		1368	4	87416	1	97591	1	5477-01	
8500		1255	4	83923	1	93692	1	6000-01	
9000		1157	4	80726	1	90123	1	6544-01	
9500		1070	4	77785	1	86840	1	7110-01	
1000	1	9935	3	75067	1	83805	1	7696-01	
1100	1	8602	3	70140	1	78304	1	8930-01	
1200	1	7544	3	65892	1	73561	1	1025	
1300	1	6678	3	62159	1	69395	1	1165	
1400	1	5923	3	58779	1	65621	1	1313	
1500	1	5334	3	55861	1	62363	1	1469	
1600	1	4782	3	53097	1	59277	1	1633	
1700	1	4322	3	50619	1	56511	1	1806	
1800	1	3919	3	48317	1	53941	1	1987	
1900	1	3540	3	46079	1	51442	1	2178	
2000	1	3207	3	43979	1	49098	1	2377	
2200	1	2630	3	40121	1	44791	1	2804	
2400	1	2180	3	36811	1	41096	1	3270	
2600	1	1834	3	34022	1	37982	1	3777	
2800	1	1558	3	31626	1	35307	1	4323	
3000	1	1337	3	29553	1	32993	1	4909	
3250	1	1117	3	27328	1	30509	1	5698	
3500	1	9438	2	25445	1	28407	1	6548	
3750	1	8064	2	23839	1	26614	1	7457	
4000	1	6958	2	22459	1	25073	1	8426	
4500	1	5316	2	20251	1	22608	1	1053	1
5000	1	4184	2	18542	1	20700	1	1284	1
5500	1	3376	2	17230	1	19236	1	1535	1
6000	1	2782	2	16190	1	18074	1	1803	1
6500	1	2334	2	15365	1	17154	1	2087	1
7000	1	1989	2	14698	1	16409	1	2385	1

TABLE A-I (Contd)

ARRIVAL TIME CALCULATIONS

λ		ΔP_s		M		U		t_{as}	
7500	1	1718	2	14146	1	15792	1	2696	1
8000	1	1501	2	13695	1	15290	1	3018	1
8500	1	1323	2	13311	1	14861	1	3349	1
9000	1	1182	2	12993	1	14506	1	3690	1
9500	1	1059	2	12718	1	14199	1	4037	1
1000	2	9615	1	12494	1	13949	1	4393	1
1100	2	8029	1	12116	1	13527	1	5121	1
1200	2	6825	1	11824	1	13201	1	5868	1
1300	2	5920	1	11599	1	12950	1	6632	1
1400	2	5186	1	11413	1	12742	1	7408	1
1500	2	4665	1	11276	1	12589	1	8198	1
1600	2	4177	1	11150	1	12448	1	8995	1
1700	2	3797	1	11052	1	12338	1	9801	1
1800	2	3488	1	10970	1	12247	1	1061	2
1900	2	3208	1	10895	1	12163	1	1143	2
2000	2	2984	1	10832	1	12093	1	1226	2
2200	2	2596	1	10726	1	11975	1	1392	2
2400	2	2299	1	10646	1	11885	1	1560	2
2600	2	2061	1	10581	1	11813	1	1728	2
2800	2	1867	1	10529	1	11755	1	1898	2
3000	2	1706	1	10485	1	11706	1	2069	2
3250	2	1537	1	10439	1	11654	1	2283	2
3500	2	1397	1	10399	1	11610	1	2498	2
3750	2	1279	1	10366	1	11572	1	2713	2
4000	2	1178	1	10337	1	11540	1	2930	2
4500	2	1015	1	10290	1	11488	1	3364	2
5000	2	8876		10254	1	11447	1	3800	2
5500	2	7857		10224	1	11415	1	4237	2
6000	2	7023		10201	1	11388	1	4676	2
6500	2	6328		10181	1	11366	1	5115	2
7000	2	5742		10164	1	11347	1	5556	2
7500	2	5222		10149	1	11331	1	5997	2
8000	2	4769		10136	1	11316	1	6438	2
9000	2	4041		10115	1	11293	1	7323	2
1000	3	3484		10100	1	11275	1	8209	2
1100	3	3047		10087	1	11261	1	9096	2
1200	3	2692		10077	1	11250	1	9985	2
1300	3	2405		10069	1	11241	1	1087	3
1400	3	2162		10062	1	11233	1	1176	3
1500	3	1970		10056	1	11227	1	1265	3
1600	3	1793		10051	1	11221	1	1355	3
1700	3	1647		10047	1	11217	1	1444	3

TABLE A-I (Contd)

ARRIVAL TIME CALCULATIONS

λ		ΔP_s	M		U		t_{as}	
1800	3	1523	10044	1	11213	1	1533	3
1900	3	1409	10040	1	11209	1	1622	3
2000	3	1314	10038	1	11206	1	1711	3
2200	3	1148	10033	1	11201	1	1890	3
2400	3	1016	10029	1	11196	1	2068	3
2600	3	9079-01	10026	1	11193	1	2247	3
2800	3	8188-01	10023	1	11190	1	2426	3
3000	3	7430-01	10021	1	11188	1	2604	3
3250	3	6640-01	10019	1	11185	1	2828	3
3500	3	5980-01	10017	1	11183	1	3051	3
3750	3	5430-01	10016	1	11181	1	3275	3
4000	3	4960-01	10014	1	11180	1	3499	3
4500	3	4200-01	10012	1	11177	1	3946	3
5000	3	3620-01	10010	1	11176	1	4393	3
5500	3	3170-01	10009	1	11174	1	4841	3
6000	3	2800-01	10008	1	11173	1	5288	3
6500	3	2500-01	10007	1	11172	1	5736	3
7000	3	2260-01	10006	1	11171	1	6183	3
7500	3	2050-01	10006	1	11171	1	6631	3
8000	3	1870-01	10005	1	11170	1	7079	3
9000	3	1580-01	10005	1	11169	1	7974	3
1000	4	1370-01	10004	1	11168	1	8869	3

Unclassified

Security Classification

DOCUMENT CONTROL DATA - R&D

(Security classification of title, body of abstract and indexing annotation must be entered when the overall report is classified)

1. ORIGINATING ACTIVITY (Corporate author) U.S. Army Ballistic Research Laboratories Aberdeen Proving Ground, Maryland	2a. REPORT SECURITY CLASSIFICATION Unclassified 2b. GROUP

3. REPORT TITLE

AIR BLAST PARAMETERS VERSUS DISTANCE FOR HEMISPHERICAL TNT SURFACE BURSTS

4. DESCRIPTIVE NOTES (Type of report and inclusive dates)

5. AUTHOR(S) (Last name, first name, initial)

Kingery, Charles N.

6. REPORT DATE	7a. TOTAL NO. OF PAGES	7b. NO. OF REFS
September 1966	81	7

8a. CONTRACT OR GRANT NO. b. PROJECT NO. c. DASA Subtask No. 01.049 d.	9a. ORIGINATOR'S REPORT NUMBER(S) Report No. 1344 9b. OTHER REPORT NO(S) (Any other numbers that may be assigned this report)

10. AVAILABILITY/LIMITATION NOTICES This document is subject to special export controls and each transmittal to foreign governments or foreign nationals may be made only with prior approval of Commanding Officer, U.S. Army Ballistic Research Laboratories, Aberdeen Proving Ground, Maryland.

11. SUPPLEMENTARY NOTES	12. SPONSORING MILITARY ACTIVITY U.S. Army Materiel Command Washington, D.C.

13. ABSTRACT

This report contains a presentation of the air blast parameters, peak overpressure, arrival time, positive duration and impulse versus scaled distances. The values of the parameters are derived from empirical measurements made on a series of tests sponsored under The Technical Cooperation Program (TTCP) i.e., Canada, the United Kingdom and the United States. The measurements were made on 5-, 20-, 100- and 500-ton TNT surface bursts. The charges consisted of small TNT blocks stacked in the shape of a hemisphere.

DD FORM 1 JAN 64 1473

Unclassified

Security Classification

Unclassified

Security Classification

14. KEY WORDS	LINK A ROLE	LINK A WT	LINK B ROLE	LINK B WT	LINK C ROLE	LINK C WT
Shock Waves						
Arrival Times						
Positive Duration						
Positive Impulse						
Peak Overpressure						

INSTRUCTIONS

1. **ORIGINATING ACTIVITY:** Enter the name and address of the contractor, subcontractor, grantee, Department of Defense activity or other organization *(corporate author)* issuing the report.

2*a*. **REPORT SECURITY CLASSIFICATION:** Enter the overall security classification of the report. Indicate whether "Restricted Data" is included. Marking is to be in accordance with appropriate security regulations.

2*b*. **GROUP:** Automatic downgrading is specified in DoD Directive 5200.10 and Armed Forces Industrial Manual. Enter the group number. Also, when applicable, show that optional markings have been used for Group 3 and Group 4 as authorized.

3. **REPORT TITLE:** Enter the complete report title in all capital letters. Titles in all cases should be unclassified. If a meaningful title cannot be selected without classification, show title classification in all capitals in parenthesis immediately following the title.

4. **DESCRIPTIVE NOTES:** If appropriate, enter the type of report, e.g., interim, progress, summary, annual, or final. Give the inclusive dates when a specific reporting period is covered.

5. **AUTHOR(S):** Enter the name(s) of author(s) as shown on or in the report. Enter last name, first name, middle initial. If military, show rank and branch of service. The name of the principal author is an absolute minimum requirement.

6. **REPORT DATE:** Enter the date of the report as day, month, year; or month, year. If more than one date appears on the report, use date of publication.

7*a*. **TOTAL NUMBER OF PAGES:** The total page count should follow normal pagination procedures, i.e., enter the number of pages containing information.

7*b*. **NUMBER OF REFERENCES:** Enter the total number of references cited in the report.

8*a*. **CONTRACT OR GRANT NUMBER:** If appropriate, enter the applicable number of the contract or grant under which the report was written.

8*b*, 8*c*, & 8*d*. **PROJECT NUMBER:** Enter the appropriate military department identification, such as project number, subproject number, system numbers, task number, etc.

9*a*. **ORIGINATOR'S REPORT NUMBER(S):** Enter the official report number by which the document will be identified and controlled by the originating activity. This number must be unique to this report.

9*b*. **OTHER REPORT NUMBER(S):** If the report has been assigned any other report numbers *(either by the originator or by the sponsor)*, also enter this number(s).

10. **AVAILABILITY/LIMITATION NOTICES:** Enter any limitations on further dissemination of the report, other than those imposed by security classification, using standard statements such as:

(1) "Qualified requesters may obtain copies of this report from DDC."

(2) "Foreign announcement and dissemination of this report by DDC is not authorized."

(3) "U. S. Government agencies may obtain copies of this report directly from DDC. Other qualified DDC users shall request through ________________."

(4) "U. S. military agencies may obtain copies of this report directly from DDC. Other qualified users shall request through ________________."

(5) "All distribution of this report is controlled. Qualified DDC users shall request through ________________."

If the report has been furnished to the Office of Technical Services, Department of Commerce, for sale to the public, indicate this fact and enter the price, if known.

11. **SUPPLEMENTARY NOTES:** Use for additional explanatory notes.

12. **SPONSORING MILITARY ACTIVITY:** Enter the name of the departmental project office or laboratory sponsoring *(paying for)* the research and development. Include address.

13. **ABSTRACT:** Enter an abstract giving a brief and factual summary of the document indicative of the report, even though it may also appear elsewhere in the body of the technical report. If additional space is required, a continuation sheet shall be attached.

It is highly desirable that the abstract of classified reports be unclassified. Each paragraph of the abstract shall end with an indication of the military security classification of the information in the paragraph, represented as *(TS)*, *(S)*, *(C)*, or *(U)*.

There is no limitation on the length of the abstract. However, the suggested length is from 150 to 225 words.

14. **KEY WORDS:** Key words are technically meaningful terms or short phrases that characterize a report and may be used as index entries for cataloging the report. Key words must be selected so that no security classification is required. Identifiers, such as equipment model designation, trade name, military project code name, geographic location, may be used as key words but will be followed by an indication of technical context. The assignment of links, rules, and weights is optional.

Unclassified

Security Classification